Springer Theses
Recognizing Outstanding Ph.D. Research

Yi Wang

Magnetic Cloud Boundary Layers and Magnetic Reconnection

Springer

Springer Theses

Recognizing Outstanding Ph.D. Research

Aims and Scope

The series "Springer Theses" brings together a selection of the very best Ph.D. theses from around the world and across the physical sciences. Nominated and endorsed by two recognized specialists, each published volume has been selected for its scientific excellence and the high impact of its contents for the pertinent field of research. For greater accessibility to non-specialists, the published versions include an extended introduction, as well as a foreword by the student's supervisor explaining the special relevance of the work for the field. As a whole, the series will provide a valuable resource both for newcomers to the research fields described, and for other scientists seeking detailed background information on special questions. Finally, it provides an accredited documentation of the valuable contributions made by today's younger generation of scientists.

Theses are accepted into the series by invited nomination only and must fulfill all of the following criteria

- They must be written in good English.
- The topic should fall within the confines of Chemistry, Physics, Earth Sciences, Engineering and related interdisciplinary fields such as Materials, Nanoscience, Chemical Engineering, Complex Systems and Biophysics.
- The work reported in the thesis must represent a significant scientific advance.
- If the thesis includes previously published material, permission to reproduce this must be gained from the respective copyright holder.
- They must have been examined and passed during the 12 months prior to nomination.
- Each thesis should include a foreword by the supervisor outlining the significance of its content.
- The theses should have a clearly defined structure including an introduction accessible to scientists not expert in that particular field.

More information about this series at http://www.springer.com/series/8790

Yi Wang

Magnetic Cloud Boundary Layers and Magnetic Reconnection

Doctoral Thesis accepted by
University of Chinese Academy of Sciences, Beijing, China

Springer

Author
Dr. Yi Wang
State Key Laboratory of Space Weather,
National Space Science Center
Chinese Academy of Sciences
Beijing
China

Supervisors
Prof. Fengsi Wei
State Key Laboratory of Space Weather,
National Space Science Center
Chinese Academy of Sciences
Beijing
China

Prof. Xueshang Feng
State Key Laboratory of Space Weather,
National Space Science Center
Chinese Academy of Sciences
Beijing
China

ISSN 2190-5053 ISSN 2190-5061 (electronic)
Springer Theses
ISBN 978-3-662-48309-1 ISBN 978-3-662-48310-7 (eBook)
DOI 10.1007/978-3-662-48310-7

Library of Congress Control Number: 2015948715

Springer Heidelberg New York Dordrecht London
© Springer-Verlag Berlin Heidelberg 2016
This work is subject to copyright. All rights are reserved by the Publisher, whether the whole or part of the material is concerned, specifically the rights of translation, reprinting, reuse of illustrations, recitation, broadcasting, reproduction on microfilms or in any other physical way, and transmission or information storage and retrieval, electronic adaptation, computer software, or by similar or dissimilar methodology now known or hereafter developed.
The use of general descriptive names, registered names, trademarks, service marks, etc. in this publication does not imply, even in the absence of a specific statement, that such names are exempt from the relevant protective laws and regulations and therefore free for general use.
The publisher, the authors and the editors are safe to assume that the advice and information in this book are believed to be true and accurate at the date of publication. Neither the publisher nor the authors or the editors give a warranty, express or implied, with respect to the material contained herein or for any errors or omissions that may have been made.

Printed on acid-free paper

Springer-Verlag GmbH Berlin Heidelberg is part of Springer Science+Business Media
(www.springer.com)

Parts of this thesis have been published in the following journal articles:

Wang, Y., Wei, F.S., Feng, X.S., Zhang, S.H., Zuo, P.B., Sun, T.R.: Energetic Electrons Associated with Magnetic Reconnection in the Magnetic Cloud Boundary Layer. Physical Review Letters 105(19), 195007 (2010). doi:10.1103/PhysRevLett.105.195007

Wang, Y., Wei, F.S., Feng, X.S., Zuo, P.B., Guo, J.P., Xu, X.J., Li, Z.: Variations of Solar Electron and Proton Flux in Magnetic Cloud Boundary Layers and Comparisons with Those across the Shocks and in the Reconnection Exhausts. The Astrophysical Journal 749(1), 82 (2012). doi:10.1088/0004-637X/749/1/82

Supervisor's Foreword

In the past two decades, space weather science has become a fast growing new field directly related with the human survival and development. However, the severe space weather events, which can do damage to our high technological systems such as satellites, navigation, electric network, and so on, are still not fully understood. How does it occur? Understanding the involved basic physical processes as well as their cause-effect chain is the main target of space weather research.

Actually, some basic energy conversion processes, such as magnetic reconnection and particle accelerations, commonly exists in space weather events. These are all important processes in the realm of physics but people do not know much about them. For example, why the energetic electrons associated magnetic reconnection are rarely observed in the solar wind? How are they accelerated? Yi Wang's thesis mainly focuses on a dynamical problem in the boundary layer of the interplanetary magnetic cloud originated from the coronal mass ejections. He found the first observational evidence of energetic electron acceleration associated with magnetic reconnection in the solar wind and proposed a combined acceleration model which includes the electric field acceleration and Fermi type mechanism. In addition, after analyzing the energy dependency and direction selectivity of particle flux variations, he suggested that particle flux variations might be an important criterion for the identification of magnetic reconnection in the solar wind.

This work is impressive because the reported first observational evidence of energetic electrons and the distinct particle flux behaviors in the boundary layer extend the idea of what we have known. Moreover, the proposed acceleration model and the possible new reconnection criterion may also have enlightenments to the understanding of the general magnetic reconnection and particle acceleration problem in the realms of solar corona, geomagnetic tail and the related astrophysics.

Beijing, China
June 2015

Prof. Fengsi Wei

Acknowledgments

I would like to express my sincere gratitude to the professors, classmates, friends, and relatives.

First and foremost, I would like to thank my supervisor Prof. Fengsi Wei and Prof. Xueshang Feng. This thesis is written under the guidance of Prof. Wei and Prof. Feng. My supervisors give me insightful instructions and valuable encouragements. Their rigorous academic attitude and profound professional knowledge are my role model.

I would like to give my thanks to the classmates and colleagues in SIGMA Weather Group, State Key Laboratory of Space Weather. I am very grateful to the collaborations and discussions with Dr. Tianran Sun, Dr. Shaohua Zhang, Dr. Shen Fang, Dr. Jianpeng Guo, Dr. Xinhua Zhao, Dr. Wenbin Song, Dr. Jiusheng Yao, Dr. Changqing Xiang, Dr. Dingkun Zhong, Dr. Yinzhi Zhang, Dr. Ming Xiong, Dr. Caoxu Liu, Dr. Chaowei Jiang, Dr. Zheng Li, and Dr. Xiaojun Xu. Special thanks go to Dr. Pingbing Zuo who teaches me basic information for the data processing. Meanwhile, I would like to thank the secretaries, Ms. Ying Fu, Ms. Jing Liang and Ms. Yuan Liu, for their help.

I would also like to thank Prof. Chuxin Chen, Prof. Quanming Lu, Prof. Mingjiu Ni, Prof. William H. Matthaeus, Dr. Tian Hui, Dr. Jiansen He, Dr. Hengqiang Feng, Dr. Lynn B. Wilson III, Dr. Zhengpeng Su, Dr. Can Huang, and Dr. Mingyu Wu for their help and assistances.

Contents

Chapter 1
Introduction

Space physics studies various physical processes that exist in different regions including the middle and high layer atmosphere, ionosphere, magnetosphere, interplanetary space, the Sun, and the entire heliosphere. With the development of modern technology, people has come to realize that the space physics is closely related to our human life. For example, the Sun releases energy all the time, and in most cases, our Earth will not be influenced if the space environment is in peace. But the Earth system is vulnerable. If the Sun quickly releases significant amount of energy and if the energy reaches our Earth, it will harm the satellites, power grids, or even human health. Such disasters are called severe space weather events which will cause unimaginably enormous damages to the developments of the modern society. Therefore, it is necessary and significant to investigate these events and take multiple actions to prevent such tragedies.

Similar to the dramatic changes in the weather, when severe space weather events happen, spacecraft would detect violent changes in the magnetic field, electric field, and the plasma conditions. This paper addresses the evolutions of drastic processes related to such events, and the main concerns are given to the realm related to magnetic reconnection and magnetic cloud boundary layer.

1.1 Magnetic Reconnection

As early as in the late 1940s, Giovanelli found that the energetic particles accelerated by the solar flare could be closely related to the magnetic reconnection (Giovanelli 1946), but he did not put forward the name as 'magnetic reconnection.' To explain the acceleration of particles in the magnetosphere, Dungey proposed the concept of magnetic reconnection (Dungey 1953). Magnetic reconnection is a physical process during which the magnetic field line 'breaks' and 'reconnects' (Fig. 1.1), and this process can convert magnetic energy into plasma thermal and kinetic energy (Birn and Priest 2007). Magnetic reconnection is a ubiquitous process existing in laboratory, space, and astrophysical contexts. During the past few decades, it becomes a hot topic in the realm of physics. Until March, 2012, more

© Springer-Verlag Berlin Heidelberg 2016

Y. Wang, *Magnetic Cloud Boundary Layers and Magnetic Reconnection*,
Springer Theses, DOI 10.1007/978-3-662-48310-7_1

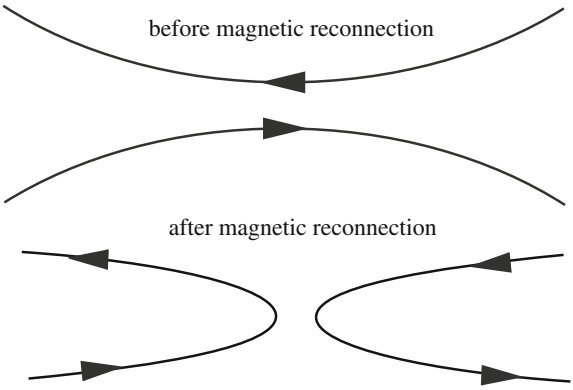

Fig. 1.1 Simple configuration of magnetic field before and after magnetic reconnection

than 20,000 scientific papers related to magnetic reconnection have been published. The basic information of magnetic reconnection will be introduced in this chapter.

Magnetic reconnection is a complex physical process that will evolve differently under different conditions. For example, magnetic reconnection process may proceed either explosively or in a steady way. It can also occur both in collisionless and collisional plasma. We would like to introduce two-dimensional reconnection models briefly to show the properties of magnetic reconnection in different environments.

1.1.1 Sweet-Parker Reconnection

Sweet (1958) and Parker (1957) proposed the first reconnection model (Fig. 1.2). Based on resistive magnetohydrodynamics (MHD) theory, the generalized Ohm's law could be written as

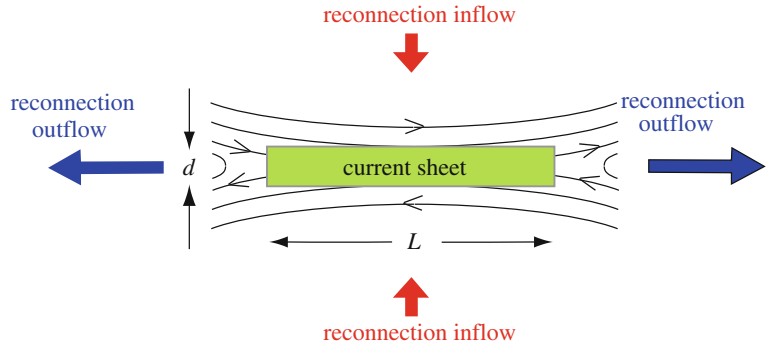

Fig. 1.2 Illustration of Sweet-Parker reconnection

$$E + V \times B = \eta J \tag{1.1}$$

The η represents resistivity, and the equation becomes ideal MHD equation if $\eta = 0$.

Figure 1.2 displays the Sweet-Parker reconnection that introduces a long and narrow current sheet (length L and with d) in which the field lines 'break' and 'reconnect.' The reconnection rate can be written as:

$$M \sim \frac{V_{in}}{V_{out}} \sim \frac{d}{L} \sim \frac{1}{\sqrt{S}} \tag{1.2}$$

where V_{in} and V_{out} denote inflow and outflow speed, respectively. S denotes the Magnetic Lundquist number which is defined as:

$$S = \frac{\mu_0 L V_A}{\eta} \tag{1.3}$$

where μ_0 is the vacuum permeability and $V_A = B/\sqrt{\mu_0 \rho}$ represents the Alfvén speed. It should be note that the Magnetic Lundquist number (S) equals to the Magnetic Reynolds number (R_m) in some cases (Huba 2004), and both of them could reveal the diffusion of the magnetic field.

The Sweet-Parker reconnection is a creative work that builds a 2D (or 2.5D) quantitative model. Since this model is based on the resistive MHD equations, and the diffusion of the magnetic field lies on the resistivity which is determined by classical collisions, Sweet-Parker reconnection is also called resistive reconnection, collisional reconnection, or slow reconnection (Cassak and Shay 2011; Daughton et al. 2009). When it is applied to the solar corona where the Magnetic Lundquist number is very large ($S > 10^6$), it is found that the calculated reconnection rate is too small to explain the observations (Parker 1957). Although Sweet-Parker reconnection requires too much time to trigger a coronal mass ejection (CME), further analyses suggest that magnetic reconnection could proceed slowly to form a long current sheet before CME in the energy build up phase. These features are properly revealed by the Sweet-Parker reconnection, and this model is widely applied in the studies of solar activities (Samtaney et al. 2009).

1.1.2 Hall Reconnection

The Earth's magnetosphere is a different place where the plasma is nearly collisionless. The magnetic field becomes frozen into the plasma. The region where magnetic reconnection occurs is a small area in the reconnection center called diffusion region (sometimes also called dissipation region, see Fig. 1.3) (Dungey 1961, 1963). This region is dominated by kinetic effects and reconnection could be initiated by the waves, plasma microinstabilities, or turbulence (Gurnett and

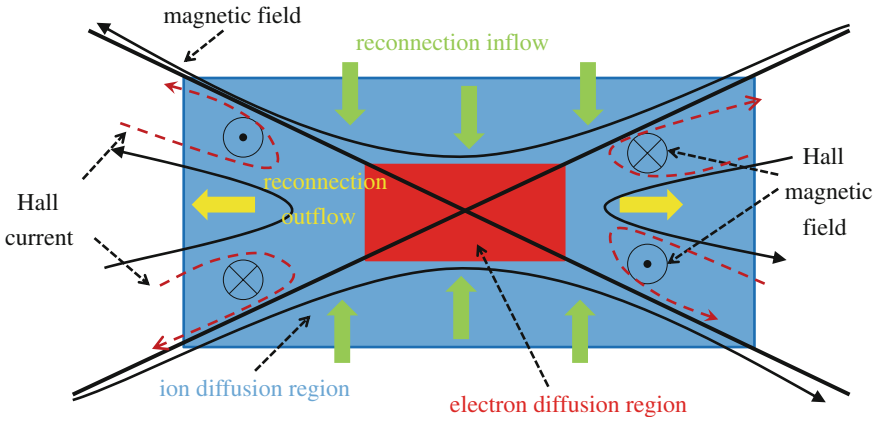

Fig. 1.3 Illustration of Hall reconnection

Bhattacharjee 2005). In such collisionless environment, the ions and electrons are not coupled inside the diffusion region, and this decouple effect controls the size of the diffusion region. The modified generalized Ohm's law in Eq. (1.4) would help understand this process (Birn and Priest 2007).

$$E + V \times B = \eta J + \frac{J \times B}{ne} - \frac{\nabla \bullet \overrightarrow{\mathbf{P}}_e}{ne} + \frac{m_e}{ne^2}\left[\frac{\partial J}{\partial t} + \nabla \bullet (JV + VJ)\right] \tag{1.4}$$

Compared with Eq. (1.1), 3 items are added to the right-hand side in Eq. (1.4). They are Hall term, the electron pressure tensor, and electronic inertia term, respectively. These terms also introduce 3 scales that are ion inertial scale $d_i = c/\omega_{pi}$, ion Larmor scale $r_l = \sqrt{T_e/m_i}/\Omega_i$ and electron inertial scale $d_e = c/\omega_{pe}$, where ω_{pi},Ω_i, ω_{pe} and c denote ion plasma frequency, Ion cyclotron frequency, electron plasma frequency, and the speed of light.

Ions and electrons are frozen into magnetic field outside the ion diffusion region in Hall reconnection. However, ions demagnetize from the magnetic field inside the ion diffusion region but electrons are still frozen to the field lines. The decouple effect between ions and electrons introduces Hall magnetic field and Hall current that control the reconnection rate. At the smaller electron diffusion region, even the electrons are demagnetized, and the dynamics are mainly controlled by the electron pressure tensor and electronic inertia term.

Generally speaking, the Hall reconnection is also called collisionless reconnection or fast reconnection in which the reconnection rate is greatly enhanced (Dungey 1961, 1963). This reconnection model is widely used in the magnetosphere such as the Geospace environmental modeling magnetic reconnection challenge (GEM) (Birn et al. 2001). Hall current and Hall magnetic field are also regarded as the typical features that are usually observed in collisionless reconnection (Øieroset et al. 2001).

1.1.3 Petschek Reconnection

In resistive reconnection, the aspect ratio of the diffusion region (d/L) controls the reconnection rate and this point could be known from Eq. (1.2). However, $d \sim S^{1/2}$ is small compared with L, which is the macro scale of the system size. As a consequence, the deduced reconnection rate is too small. To enhance the reconnection rate, Petschek (1964) proposed a revised model in which the length of the diffusion region is much shorter. In Petschek mode, the reconnection diffusion region is limited in a small region and two pairs of slow mode shocks which could heat and accelerate the plasma are introduced (see Fig. 1.4). In such a frame work, the reconnection rate is greatly boosted and the calculated maximum reconnection rate is $M = \pi/(8 \ln S)$.

Numerical simulations indicate that Petschek reconnection cannot be sustained and it will transform to Sweet-Park reconnection if the resistivity is uniform throughout the region (Uzdensky and Kulsrud 2000). Petschek-like reconnection assumes that the resistivity increases sharply in the X-shape center region where the current density is high. This diffusion region is small and there is a pair of V-shape reconnection outflow regions at both sides. Theses outflow regions are often observed in the solar wind and they are also called reconnection exhausts (Gosling 2011; Gosling et al. 2005b; Phan et al. 2006). Spacecraft will detect back to back Alfvén waves if it crosses the Petschek-like reconnection exhaust (Fig. 1.5).

1.1.4 Open Questions

In the past few decades, a lot of work have been done by the scholars on the subjects of magnetic reconnection in the solar corona and magnetosphere, but

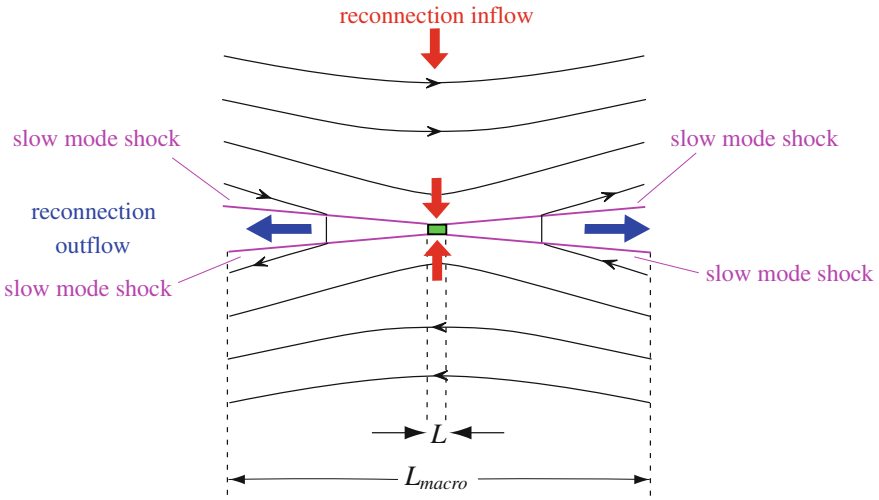

Fig. 1.4 Illustration of Petschek reconnection

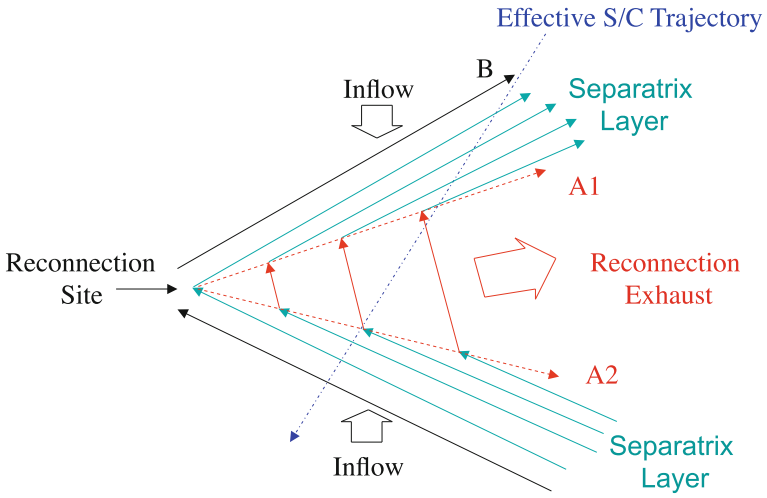

Fig. 1.5 Petschek-like reconnection exhaust. Reprinted from (Gosling 2011), with kind permission from Springer Science + Business Media

reconnection in the solar wind (interplanetary space) received relatively less attention. The solar wind has a typical velocity of $\sim$400 km/s around 1AU, while the ion inertial scale is $\sim$100 km. It is difficult for current spacecraft with limited resolution to detect the reconnection diffusion region where there are various physical processes. Therefore, the absence of detailed observations in the reconnection diffusion region make it hard for scholars to carry out more insightful analyses. In addition, solar wind is full of turbulence. Typical reconnection signatures observed by the spacecraft, such as the reconnection jets, might be mixed with the turbulent fluctuations (Wei et al. 2003a, b, c). It is very interesting to discuss the reconnection behaviors in these complex regions.

1.2 Particle Acceleration in Magnetic Reconnection

Parts of energy released in magnetic reconnection are transported to the accelerated particles. It is found that up to 50 % of the energy can be released to accelerate 20–100 keV electrons during the reconnection in the solar flares (Lin and Hudson 1971). Direct observation of electrons accelerated up to 300 keV by magnetic reconnection in the Earth's magnetotail has also been reported (Øieroset et al. 2002). According to MHD simulations, the bulk velocity of the electrons could only be boosted to the order of Alfvén speed. How the electrons are accelerated to hundreds of Kilo Electron Volt is a controversial topic (Ambrosiano et al. 1988; Birn et al. 2000, 2004; Blackmana and Field 1994; Dmitruk et al. 2004; Drake et al. 2003, 2006; Egedal et al. 2012; Goldstein et al. 1986; Hoshino 2005, 2012;

Hoshino et al. 2001; Imada et al. 2007; Matthaeus et al. 1984; Möbius et al. 1983; Oka et al. 2010a, b; Pritchett 2006a, b, 2008; Wang et al. 2010).

1.2.1 Acceleration Region and Acceleration Process

Observations from the Geotail and Cluster spacecraft indicate that the accelerated electrons are more often found in the reconnection outflow region but not in the diffusion region (Imada et al. 2005, 2007). However, observations from the WIND spacecraft show that the fluxes of the accelerated energetic electrons[1] peak near the center of the diffusion region and decrease monotonically away from this region (Fig. 1.6) (Øieroset et al. 2002).

These inconsistent observations also lead to another dispute about the acceleration processes. Some authors indicate that the electrons are preliminarily accelerated in the diffusion region and then mainly accelerated to high energy in the outflow region (Hoshino et al. 2001; Imada et al. 2007). Observations show that the energy spectrum of the energetic electrons is harder[2] in the outflow region (Imada et al. 2007), and the spectrums with double power law are also found in magnetic reconnection (Lin et al. 2003). These evidences seem to support the concept of two-step acceleration. However, observations of electron fluxes from the WIND spacecraft indicate that the electrons are accelerated in the diffusion region (Øieroset et al. 2002). It is found that the power index varies the same as the fluxes. The hardest spectrum is located in the diffusion region and spectrum becomes softer as the distance increases away from the reconnection center. No evidence of two-step acceleration has been found.

1.2.2 Acceleration Mechanism

Direct acceleration by the electric field is the simplest case. As shown in Fig. 1.7, if an ideal 2.5D reconnection model is assumed in the magnetotail, there exists a reconnection electric field (E) pointing to the dawn-dusk direction. When a particle moves along this electric field with a distance L, it will gain the potential energy $W = EL$ (Möbius et al. 1983). This energy could be roughly estimated to be

[1] *Note* The reconnection accelerated electrons with high energy (usually greater than 1 keV) are also called nonthermal electron or suprathermal electron by some authors. However, 100–700 eV electrons in the solar wind, which is often used to diagnose the magnetic field, are also called suprathermal electron. Here we use energetic electron to denote the reconnection accelerated electron with high energy (usually greater than 1 keV).

[2] *Note* The electron flux spectrum usually obeys a power law at high-energy range. The relation between the phase space density and energy can be descripted by $f \sim E^{-k}$. A smaller power index k means a harder spectrum.

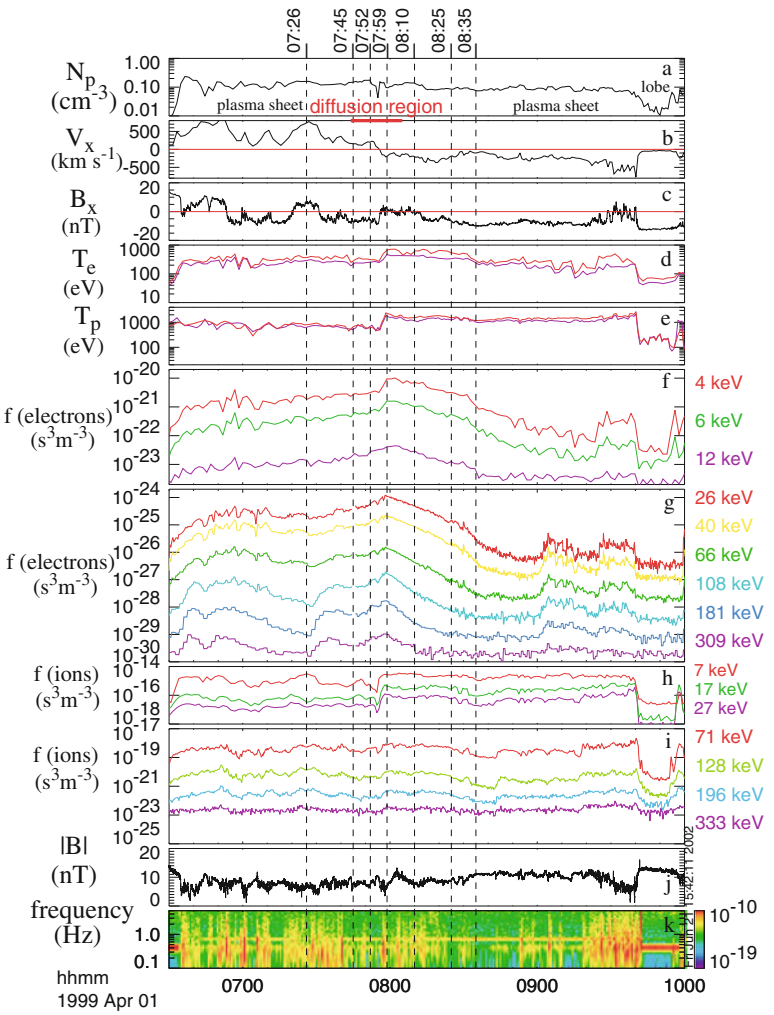

Fig. 1.6 The fluxes of the energetic electrons accelerated by magnetic reconnection. Reprinted with permission from (Øieroset et al. 2002). Copyright 2002 by American Physical Society

$\sim$200 keV (Birn and Priest 2007). In this framework, the ions and electrons would move in different directions in the same electric field, and there should be a dawn-dusk asymmetric distribution of the accelerated particles. But this phenomenon is not very distinct as is expected (Imada et al. 2002, 2008). In addition, a power law spectrum of the energetic particles requires the electric field increase exponentially in time (Deeg et al. 1991; Zelenyi et al. 1990). But this condition is not satisfied in this simple model. Actually, particles would run away from the acceleration region before they are accelerated to such high energy. Therefore, the acceleration of energetic particles is not a single process, there should exist a

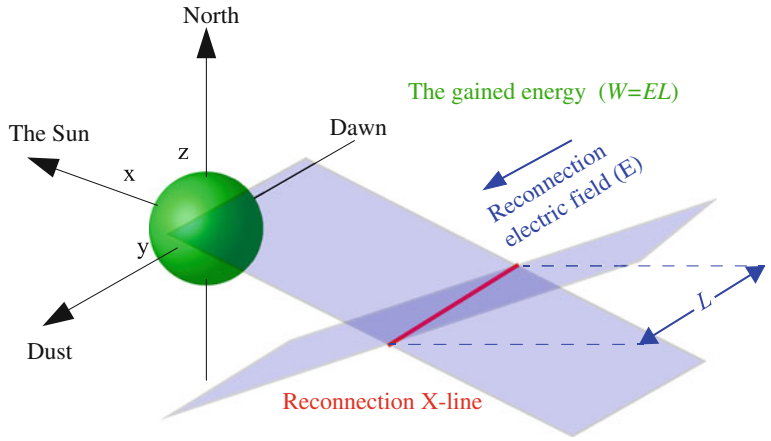

Fig. 1.7 Direct acceleration by reconnection electric field

mechanism which could trap the particles in the acceleration region so that the particles have enough time to be accelerated (Fujimoto and Machida 2003; Hoshino 2005, 2012; Hoshino et al. 2001; Oka et al. 2010a).

Besides the reconnection electric field, particles would also be accelerated by the electric field generated by various waves associated with magnetic reconnection. The broadband electrostatic noise (Lakhina et al. 2000; Matsumoto et al. 1994; Omura et al. 1994) (BEN) whose frequency extends broadly from the lower hybrid frequency to the plasma frequency could be usually observed in the magnetotail. By analyzing the high resolution data, a series of electrostatic solitary waves (Huttunen et al. 2007; Ng et al. 2006; Omura et al. 1994; Wilson et al. 2007) (ESW) are discriminated from the BEN. The scale of these ESWs is in an order of 10 Debye length, and their amplitude could be 100 times larger than the reconnection electric field. So this electric field could provide considerable energy to accelerate electrons. Numerical simulations also suggest that the electron holes formed near the reconnection separatrix could generate strong electric field by which ions are scattered and accelerated (Drake et al. 2003).

Charged particles would undergo repeated reflections under specified configuration of magnetic field, such as in the magnetic island. Under high Lundquist number condition, if the reconnection current sheet is long enough, instabilities would lead the formation of magnetic islands instead of a single X-line. It provides favorable conditions for Fermi-type acceleration (Fig. 1.8).

Fermi acceleration could be classified into two types. The electrons would undergo an efficient first-order Fermi acceleration process and gain energy when bouncing in a contracting magnetic island. They could also boost their energy via second-order Fermi acceleration by bouncing among the magnetic islands (Drake et al. 2006). Analyses show that the energetic electrons would reveal a power law spectrum after Fermi acceleration, and this scenario also consists with the observations. However, the electrons get less energy if the contractions of the magnetic

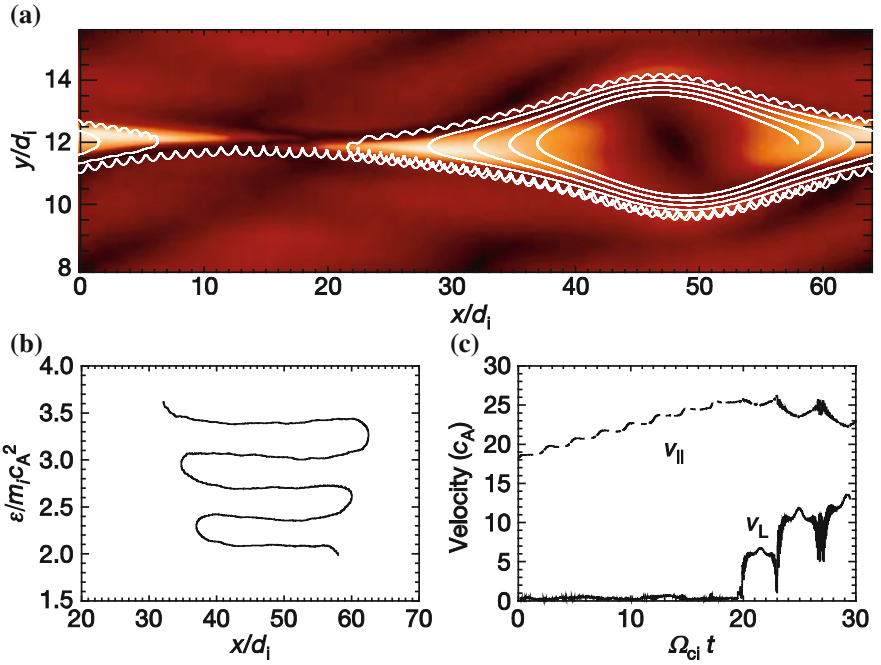

Fig. 1.8 Fermi acceleration in magnetic reconnection. Reprinted by permission from Macmillan Publishers Ltd: (Drake et al. 2006), copyright 2006

island is blocked by the plasma pressure. Therefore, it should be noted that the proposed Fermi mechanism is less efficient in high beta plasma (beta is the ratio of the plasma pressure to the magnetic pressure) (Drake et al. 2006).

Microinstabilities could occur and various waves could be generated near the reconnection region. If the velocity of a particle approximately equals to the phase velocity v_p of the electromagnetic wave, Landau damping would occur. Particles with velocities $v_p - \Delta V$ would gain energy from the wave and be accelerated, while the other particles with velocities $v_p + \Delta V$ would lose energy to the wave and be decelerated. To collisionless plasma, since the distribution of phase space density is close to the Maxwellian distribution, as seen in Fig. 1.9, the number of particles with velocities slightly less than v_p is always greater than the number of particles with velocities slightly greater. So overall, particles would get accelerated via wave particle interactions (Malmberg and Wharton 1964).

In some cases, particles could be accelerated by the betatron acceleration (Birn et al. 2000). In the magnetotail, the first adiabatic invariant (magnetic moment) is approximately a constant: $\mu = (mv_\perp^2)/2B$. When a particle leaves the reconnection diffusion region and moves to the Earth, its perpendicular velocity $v_\perp$ would be boosted due to the sudden change in the magnetic field B. In addition, the second adiabatic invariant (longitudinal invariant $J = \int mv_\parallel dl$) is also an adiabatic invariant. Thus particles could also be heated in the parallel direction via first-order

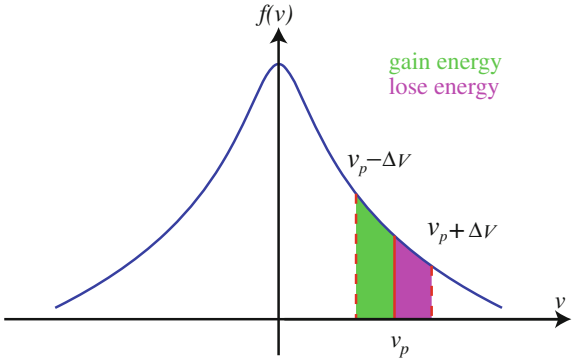

Fig. 1.9 Illustration of Landau damping

Fermi acceleration. If the magnetic field line becomes shooter when the particle bounces in the magnetic mirror, the parallel velocity $v_{\|}$ of the particle would increase (Birn and Priest 2007). Moreover, turbulence, shocks, and other quasi-Fermi acceleration models are usually involved when discussing particle acceleration problem (Ambrosiano et al. 1988; Blackman and Field 1994; Goldstein et al. 1986; Matthaeus et al. 1984). The acceleration of energetic particles tends to be a complex processes combined with different mechanisms.

1.2.3 Open Questions

Magnetic reconnection is generally regarded as an efficient accelerator to produce energetic particles, and this opinion is confirmed by the observations in the magnetotail and solar corona. However, it is so surprising that energetic particles are rarely observed in solar wind magnetic reconnection exhausts (Gosling et al. 2005a). Canot they be produced in solar wind magnetic reconnection? Or they are indeed produced but just not observed? Therefore, it is significant to analyze the energetic particle acceleration associated with magnetic reconnection in the solar wind.

1.3 Magnetic Cloud Boundary Layer

Magnetic cloud (MC), a subset of the interplanetary coronal mass ejection (ICME), is a large-scale transient structure observed in the solar wind. In the past few decades, its solar origin, magnetic field, and plasma structures have been widely discussed. In the MC body, the magnitude of the magnetic field usually increases, the magnetic field vector usually reveals smooth rotation, and the proton temperature usually decreases (Bothmer and Schwenn 1994; Burlaga et al. 1980, 1981; Burlaga 1995; Farrell et al. 2002; Lepping et al. 1997, 2006). The propagation of

MC in solar wind is an interesting topic. For example, a MC could be overtaken by a corotating stream so that the plasma and magnetic field in the tail region of the MC would be compressed and become turbulent (Lepping et al. 1997). In addition, there might also exist magnetic holes, directional discontinuities, or reconnection layers in front of a MC (Janoo et al. 1998). Therefore, the interactions between the MC body and the ambient solar wind is a complex problem which not only aggravates the difficulty to understand the evolutions of ICME but also increases the complexity to identify the MC boundary (Wei et al. 2003b).

1.3.1 The Identification of MC Boundary

There has been no consistency among the criteria identifying the MC boundary so far (Burlaga 1995). For example, the bidirectional suprathermal electron could be a useful signature to determine the MC boundary, but it can not be observed in every MC boundary. Neither can the other signatures, such as temperature decrease, density decrease, directional discontinuity, or magnetic hole. These features could occur near the MC boundary but they reveal inconsistencies in time. Wei et al. (2003b) statistically analyzed 80 MC events from 1969 to 2001 and presented the concept of MC boundary layer (BL). As seen in Fig. 1.10, rather than a simple discontinuity, the BL is a dynamical layer formed by the interactions between the MC and the background solar wind. The inner boundaries of the BL at the MC-side (G_f and G_t) are just the beginning and the end of MC body, while the outer boundaries (M_f and M_t) are determined by systematic analyses of the magnetic field and plasma signatures (Wei et al. b, 2003c, 2006).

1.3.2 Properties of the BL

Previous statistical analyses have macroscopically focused on the characteristics of the magnetic field, plasma as well as the wave activities (Wei et al. 2003a, b, c, 2005, 2006).

The BL is a non-pressure-balanced structure. The increase of thermal pressure in the BL often cannot compensate the decrease of magnetic pressure, so that the total pressure (thermal pressure plus magnetic pressure) in the BL is usually lower than that in the ambient solar wind (Wei et al. 2006). Compared with those in the nearby upstream solar wind, the magnetic field in the BL is decreased and the plasma is compressed and heated. These features are similar to the signatures of magnetic reconnection. Numerical simulations also suggest that magnetic reconnection could probably occur in the BL (Fig. 1.11).

Magnetic structures inside BL are also studied (Wei et al. 2003c). It is found that (1) the distribution functions of fluctuations in the southward magnetic field component ($\triangle$Bz) inside the boundary layer is distinct from those in the background

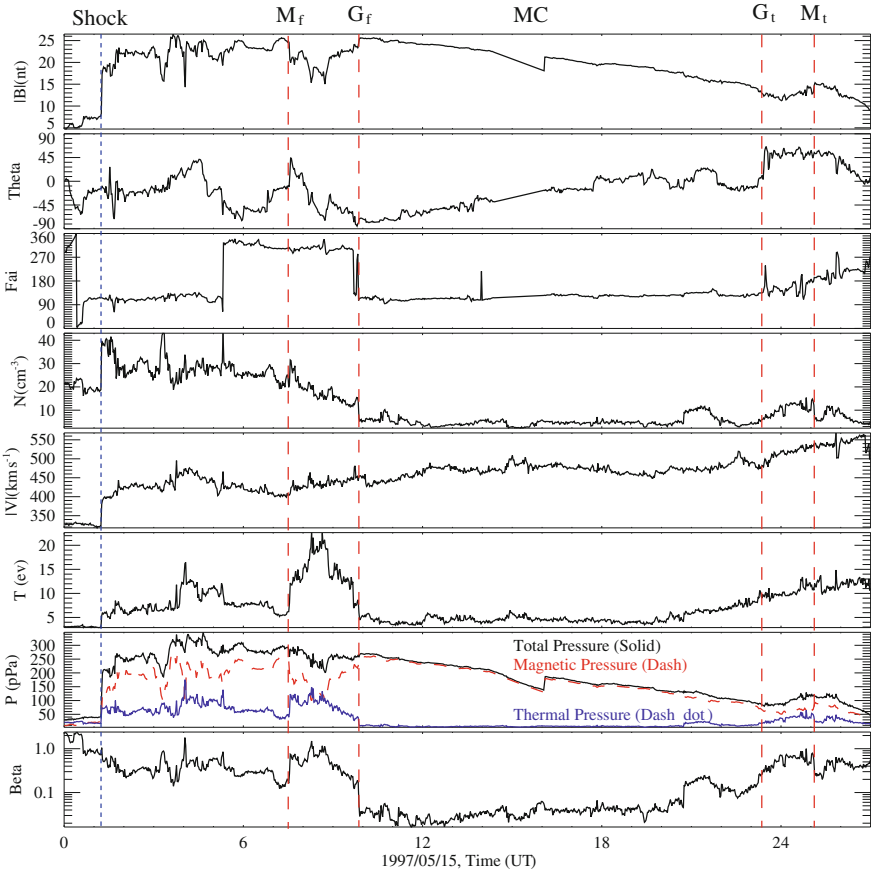

Fig. 1.10 Wind measurements of the magnetic field strength, latitude angle (ϕ), azimuth angle (θ), proton density, temperature, velocity, pressure, and plasma beta value in a MC event. The *red dashed lines* denote the front BL (between M_f and G_f) and tail BL (between M_t and G_t). The *blue dashed line* denotes shock

solar wind, and the fluctuation amplitude of ΔBz is also larger in the BL; (2) circle arc and random walk distributions in the maximum variance plane, which could imply the Alfvén fluctuations and turbulence, are usually found in the BL; (3) the distribution of magnetic field in the ϕ-θ plane exhibits a 'U' or inverse 'U' shape with a spacing of about 180° in the azimuthal angle. This feature could also indicate the existence of field reversal region and the associated Alfvénic fluctuations.

In addition, wave activities inside the BL are statistically analyzed (Wei et al. 2005). By analyzing 60 BL events observed by the WIND thermal noise receptor (TNR) instrument, it is found that there are often various plasma wave activities in the BL, which are different from those in the ambient solar wind and the MC (Fig. 1.12). The Langmuir wave near the electronic plasma frequency is always enhanced in 75 % of the investigated events. In 60 % of the total events, the

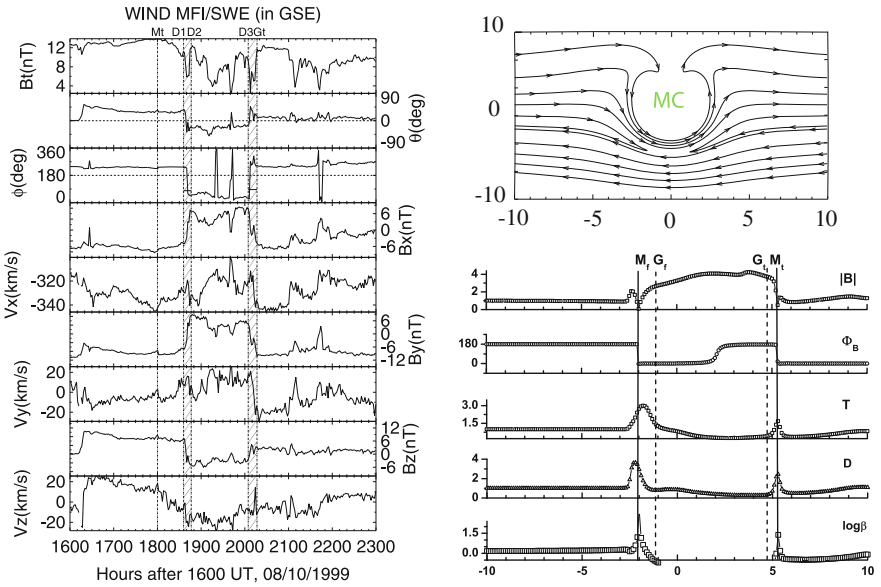

Fig. 1.11 (*Left*) The *dashed* regions show properties of magnetic reconnection. Reproduced from (Wei et al. 2006) by permission of John Wiley and Sons Ltd. (*Right*) Numerical simulation of interactions between MC and the ambient solar wind Reproduced from (Wei et al. 2003b) by permission of John Wiley and Sons Ltd

enhancement of Langmuir wave and ion acoustic wave are both observed at the same time. It is also found that the broadband wave activities, which are analogous to the BEN in the magnetotail, could be also observed in 75 % of the investigated events.

1.3.3 Open Questions

The solar activities might influence the properties of the BL. However, as time goes by, the accumulated data make it possible to eliminate this potential influences. So analyzing the properties of the BL through an entire solar circle could be an interesting work. Moreover, previous work demonstrated that magnetic reconnection could prevail in the BL. But BL is a turbulent region in which the macroscopic reconnection signatures, such as the changes in magnetic field and plasma, might not be very obvious to be observed. In addition, it is also important to know the microscopic properties, such as the variations of particle flux, in the BL and it could be very significant if the flux variations could be related to the reconnection processes.

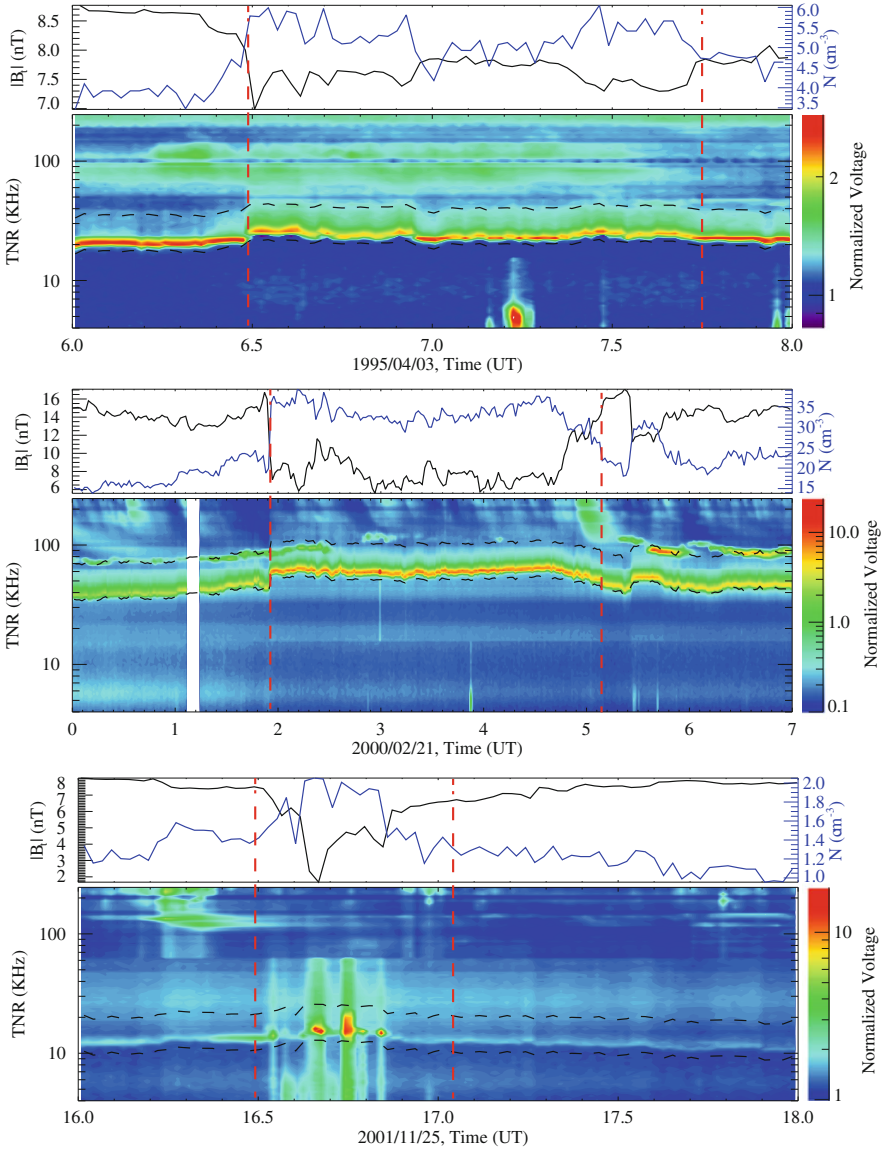

Fig. 1.12 WIND TNR spectrum: Langmuir wave, ion acoustic wave and broadband waves in the BL. The *red dashed lines* mark the BL region and the *black dashed lines* denote the local electronic plasma frequency and its harmonic

1.4 Magnetic Reconnection in the Solar Wind

Early scholars tend to use the change of magnetic field and plasma parameters, such as the reversed direction of magnetic field, reversed plasma flow and sharp increase of plasma temperature, to determinate the interplanetary magnetic reconnection. These characteristics are indeed consistent with the theoretical model of magnetic reconnection, and sometimes they can also be observed simultaneously in certain events; however, Gosling (2011) regards that the 'direct evidence' of magnetic reconnection in the solar wind should be the roughly Alfvénic accelerated jets embedded within bifurcated current sheets (Gosling 2011; Gosling et al. 2005b). As seen in Fig. 1.5, if a spacecraft crosses a reconnection exhaust, it would observe the Alfvénic disturbances propagating parallel and anti-parallel to B successively. Such anti-correlated and correlated changes in V and B are strong signatures of reconnection jets.[3]

1.4.1 Structure of the Reconnection Exhaust

Generally, the reconnection exhaust is often assumed to have an X-type structure (Fig. 1.13). According to multiple-spacecraft observations, magnetic reconnection in the solar wind is a large-scale process. Near 1 AU, the reconnection X-line could extend to hundreds of Earth radii (Re) (Phan et al. 2006), and the reconnection jets could extend $\sim 4.26 \times 10^6$ km far away from the X-line (Gosling et al. 2007a). In addition, the oppositely directed jets from the X-line were observed (Davis et al. 2006; Xu et al. 2011), and the boundaries of the exhausts were found to be roughly planar (Phan et al. 2006).

1.4.2 Physical Properties of Magnetic Reconnections in the Solar Wind

Magnetic reconnections in the solar wind have been demonstrated to be Petchek-like reconnection, and its reconnection rate is typically 3–5 % (Davis et al. 2006; Gosling et al. 2005b; Phan et al. 2006; Wang et al. 2010). Although it is fast reconnection, the Hall signatures associated with such reconnections have not been found yet. One possible reason could be that the observational location of the spacecraft is far away from the X-line ($>10^5 d_i$) so that the Hall magnetic field decays. Another reason may be attributed to the large guide field in these events,

[3]*Note* These reconnection jets could be described by the 'Walen' relation which would be discussed in Chaps. 2 and 5.

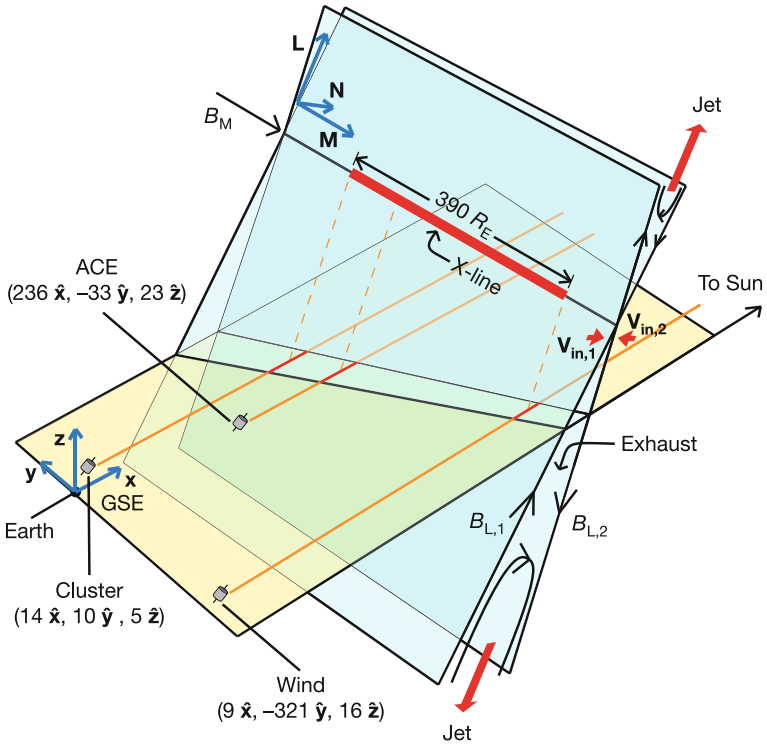

Fig. 1.13 Large-scale reconnection exhaust observed near 1 AU. Reprinted by permission from Macmillan Publishers Ltd: (Phan et al. 2006), copyright 2006

since it is not very easy to distinguish the weak Hall signatures from the overlapped large guide field.

Statistical work also reveals that magnetic reconnection in the solar wind prefers to occur in low beta value solar wind, and it could initiate spontaneously. The occurrence of magnetic reconnection in the solar wind could be very high. WIND spacecraft has once observed $\sim$1.5 times reconnection events per day in March 2006 (Gosling et al. 2007b). In addition, such reconnection tends to be quasi-steady and large-scale (Gosling 2011; Gosling et al. 2007a, b), and observations indicate that the reconnection exhaust could persist for hours.

1.4.3 Open Questions

The Alfvénic reconnection jets have been widely used to determinate magnetic reconnection events in the solar wind (Gosling 2011). However, in some regions, such as in the BL, the local environment is in a turbulent status, thus it might be difficult to identify the roughly Alfvénic jets (Wang et al. 2012; Wei et al. 2003b).

How to properly discriminate the reconnection processes in such cases? If no roughly Alfvénic accelerated plasma flows been found, does it mean that no magnetic reconnection occurs? Could other quantities be used to determinate magnetic reconnection? These questions could be very meaningful.

References

Ambrosiano, J., Matthaeus, W.H., Goldstein, M.L., Plante, D.: Test particle acceleration in turbulent reconnecting magnetic fields. J. Geophys. Res. **93**(A12), 14383–14400 (1988). doi:10.1029/JA093iA12p14383

Birn, J., Drake, J.F., Shay, M.A., Rogers, B.N., Denton, R.E., Hesse, M., Kuznetsova, M., Ma, Z. W., Bhattacharjee, A., Otto, A., Pritchett, P.L.: Geospace environmental modeling (GEM) magnetic reconnection challenge. J. Geophys. Res. **106**(A3), 3715–3719 (2001). doi:10.1029/1999ja900449

Birn, J., Priest, E.R.: Reconnection Of Magnetic Fields: Magnetohydrodynamics and Collisionless Theory and Observations. Cambridge University Press, Cambridge (2007)

Birn, J., Thomsen, M.F., Borovsky, J.E., Reeves, G.D., Hesse, M.: Particle acceleration in the dynamic magnetotail. Phys. Plasmas **7**(5), 2149–2156 (2000). doi:10.1063/1.874035

Birn, J., Thomsen, M.F., Hesse, M.: Electron acceleration in the dynamic magnetotail: test particle orbits in three-dimensional magnetohydrodynamic simulation fields. Phys. Plasmas **11**(5), 1825–1833 (2004). doi:10.1063/1.1704641

Blackman, E.G., Field, G.B.: Nonthermal acceleration from reconnection shocks. Phys. Rev. Lett. **73**(23), 3097–3100 (1994). doi:10.1103/PhysRevLett.73.3097

Bothmer, V., Schwenn, R.: Eruptive prominences as sources of magnetic clouds in the solar wind. Space Sci. Rev. **70**(1), 215–220 (1994). doi:10.1007/bf00777872

Burlaga, L., Lepping, R., Weber, R., Armstrong, T., Goodrich, C., Sullivan, J., Gurnett, D., Kellogg, P., Keppler, E., Mariani, F., Neubauer, F., Rosenbauer, H., Schwenn, R.: Interplanetary particles and fields, November 22 to December 6, 1977: helios, voyager, and imp observations between 0.6 and 1.6 AU. J. Geophys. Res. **85**(A5), 2227–2242 (1980). doi:10.1029/JA085iA05p02227

Burlaga, L., Sittler, E., Mariani, F., Schwenn, R.: Magnetic loop behind an interplanetary shock: voyager, helios, and IMP 8 observations. J. Geophys. Res. **86**(A8), 6673–6684 (1981). doi:10.1029/JA086iA08p06673

Burlaga, L.F.: Interplanetary Magnetohydrodynamics. Oxford Univ. Press, New York (1995)

Cassak, P.A., Shay, M.A.: Magnetic Reconnection for Coronal Conditions: Reconnection Rates, Secondary Islands and Onset. Space Sci. Rev. 1–20 (2011). doi:10.1007/s11214-011-9755-2

Daughton, W., Roytershteyn, V., Albright, B.J., Karimabadi, H., Yin, L., Bowers, K.J.: Transition from collisional to kinetic regimes in large-scale reconnection layers. Phys. Rev. Lett. **103**(6), 065004 (2009). doi:10.1103/PhysRevLett.103.065004

Davis, M.S., Phan, T.D., Gosling, J.T., Skoug, R.M.: Detection of oppositely directed reconnection jets in a solar wind current sheet. Geophys. Res. Lett. **33**(19), L19102 (2006). doi:10.1029/2006gl026735

Deeg, H.-J., Borovsky, J.E., Duric, N.: Particle acceleration near X-type magnetic neutral lines. Phys. Fluids B **3**(9), 2660–2674 (1991). doi:10.1063/1.859978

Dmitruk, P., Matthaeus, W.H., Seenu, N.: Test particle energization by current sheets and nonuniform fields in magnetohydrodynamic turbulence. Astrophys. J. **617**(1), 667 (2004). doi:10.1086/425301

Drake, J.F., Swisdak, M., Cattell, C., Shay, M.A., Rogers, B.N., Zeiler, A.: Formation of electron holes and particle energization during magnetic reconnection. Science **299**(5608), 873–877 (2003). doi:10.1126/science.1080333

Drake, J.F., Swisdak, M., Che, H., Shay, M.A.: Electron acceleration from contracting magnetic islands during reconnection. Nature **443**(7111), 553–556 (2006). doi:10.1038/nature05116

Dungey, J.W.: Conditions for the occurrence of electrical discharges in astrophysical systems. Phil. Mag. **44**(354), 725–738 (1953)

Dungey, J.W.: Interplanetary magnetic field and the auroral zones. Phys. Rev. Lett. **6**(2), 47–48 (1961). doi:10.1103/PhysRevLett.6.47

Dungey, J.W.: The structure of the exosphere or adventures in velocity space. In: DeWitt, C., Hieblot, J., LeBeau, L. (eds.) Geophysics, The Earth's Environment, vol. 503. Gordon and Breach, New York (1963)

Egedal, J., Daughton, W., Le, A.: Large-scale electron acceleration by parallel electric fields during magnetic reconnection. Nature Phys. **8**(4), 321–324 (2012). doi:10.1038/nphys2249

Farrell, W.M., Desch, M.D., Kaiser, M.L., Goetz, K.: The dominance of electron plasma waves near a reconnection X-line region. Geophys. Res. Lett. **29**(19), 1902 (2002). doi:10.1029/2002gl014662

Fujimoto, K., Machida, S.: An electron heating mechanism in the outflow region from the X-type neutral line. J. Geophys. Res. **108**(A9), 1349 (2003). doi:10.1029/2002ja009810

Giovanelli, R.G.: A theory of chromospheric flares. Nature **158**(4003), 81–82 (1946). doi:10.1038/158081a0

Goldstein, M.L., Matthaeus, W.H., Ambrosiano, J.J.: Acceleration of charged particles in magnetic reconnection: Solar flares, the magnetosphere, and solar wind. Geophys. Res. Lett. **13**(3), 205–208 (1986). doi:10.1029/GL013i003p00205

Gosling, J.T.: Magnetic Reconnection in the Solar Wind Space Sci. Rev. 1–14 (2011). doi:10.1007/s11214-011-9747-2

Gosling, J.T., Eriksson, S., Blush, L.M., Phan, T.D., Luhmann, J.G., McComas, D.J., Skoug, R. M., Acuna, M.H., Russell, C.T., Simunac, K.D.: Five spacecraft observations of oppositely directed exhaust jets from a magnetic reconnection X-line extending $> 4.26 \times 10^6$ km in the solar wind at 1 AU. Geophys. Res. Lett. **34**(20), L20108 (2007a). doi:10.1029/2007gl031492

Gosling, J.T., Phan, T.D., Lin, R.P., Szabo, A.: Prevalence of magnetic reconnection at small field shear angles in the solar wind. Geophys. Res. Lett. **34**(15), L15110 (2007b). doi:10.1029/2007gl030706

Gosling, J.T., Skoug, R.M., Haggerty, D.K., McComas, D.J.: Absence of energetic particle effects associated with magnetic reconnection exhausts in the solar wind. Geophys. Res. Lett. **32**(14), L14113 (2005a). doi:10.1029/2005gl023357

Gosling, J.T., Skoug, R.M., McComas, D.J., Smith, C.W.: Direct evidence for magnetic reconnection in the solar wind near 1 AU. J. Geophys. Res. **110**(A1), A01107 (2005b). doi:10.1029/2004ja010809

Gurnett, D.A., Bhattacharjee, A.: Introduction to Plasma Physics: With Space and Laboratory Applications. Cambridge University Press, Cambridge (2005)

Hoshino, M.: Electron surfing acceleration in magnetic reconnection. J. Geophys. Res. **110**(A10), A10215 (2005). doi:10.1029/2005ja011229

Hoshino, M.: Stochastic particle acceleration in multiple magnetic islands during reconnection. Phys. Rev. Lett. **108**(13), 135003 (2012). doi:10.1103/PhysRevLett.108.135003

Hoshino, M., Mukai, T., Terasawa, T., Shinohara, I.: Suprathermal electron acceleration in magnetic reconnection. J. Geophys. Res. **106**(A11), 25979–25997 (2001). doi:10.1029/2001ja900052

Huba, J.D.: NRL Plasma Formulary. Revised. Naval Research Laboratory, Washington, DC (2004)

Huttunen, K.E.J., Bale, S.D., Phan, T.D., Davis, M., Gosling, J.T.: Wind/WAVES observations of high-frequency plasma waves in solar wind reconnection exhausts. J. Geophys. Res. **112**(A1), A01102 (2007). doi:10.1029/2006ja011836

Imada, S., Hoshino, M., Mukai, T.: The dawn-dusk asymmetry of energetic and thermal electrons: the Geotail observations. In: Winglee, R.M. (ed.) Substorms-5, pp. 388–393. University of Washington, Seattle (2002)

Imada, S., Hoshino, M., Mukai, T.: Average profiles of energetic and thermal electrons in the magnetotail reconnection regions. Geophys. Res. Lett. **32**(9), L09101 (2005). doi:10.1029/2005gl022594

Imada, S., Hoshino, M., Mukai, T.: The dawn-dusk asymmetry of energetic electron in the Earth's magnetotail: Observation and transport models. J. Geophys. Res. **113**(A11), A11201 (2008). doi:10.1029/2008ja013610

Imada, S., Nakamura, R., Daly, P.W., Hoshino, M., Baumjohann, W., Mühlbachler, S., Balogh, A., Rème, H.: Energetic electron acceleration in the downstream reconnection outflow region. J. Geophys. Res. **112**(A3), A03202 (2007). doi:10.1029/2006ja011847

Janoo, L., Farrugia, C.J., Torbert, R.B., Quinn, J.M., Szabo, A., Lepping, R.P., Ogilvie, K.W., Lin, R.R., Larson, D., Scudder, J.D., Osherovich, V.A., Steinberg, J.T.: Field and flow perturbations in the October 18-19, 1995, magnetic cloud. J. Geophys. Res. **103**(A8), 17249–17259 (1998). doi:10.1029/97ja03173

Lakhina, G.S., Tsurutani, B.T., Kojima, H., Matsumoto, H.: "Broadband" plasma waves in the boundary layers. J. Geophys. Res. **105**(A12), 27791–27831 (2000). doi:10.1029/2000ja900054

Lepping, R.P., Berdichevsky, D.B., Wu, C.C., Szabo, A., Narock, T., Mariani, F., Lazarus, A.J., Quivers, A.J.: A summary of WIND magnetic clouds for years 1995-2003: model-fitted parameters, associated errors and classifications. Ann. Geophys. **24**(1), 215–245 (2006). doi:10.5194/angeo-24-215-2006

Lepping, R.P., Burlaga, L.F., Szabo, A., Ogilvie, K.W., Mish, W.H., Vassiliadis, D., Lazarus, A.J., Steinberg, J.T., Farrugia, C.J., Janoo, L., Mariani, F.: The Wind magnetic cloud and events of October 18-20, 1995: Interplanetary properties and as triggers for geomagnetic activity. J. Geophys. Res. **102**(A7), 14049–14063 (1997). doi:10.1029/97ja00272

Lin, R.P., Hudson, H.S.: 10–100 keV electron acceleration and emission from solar flares. Sol. Phys. **17**(2), 412–435 (1971). doi:10.1007/bf00150045

Lin, R.P., Krucker, S., Hurford, G.J., Smith, D.M., Hudson, H.S., Holman, G.D., Schwartz, R.A., Dennis, B.R., Share, G.H., Murphy, R.J., Emslie, A.G., Johns-Krull, C., Vilmer, N.: RHESSI observations of particle acceleration and energy release in an intense solar gamma-ray line flare. Astrophys. J. Lett. **595**(2), L69 (2003). doi:10.1086/378932

Möbius, E., Scholer, M., Hovestadt, D., Paschmann, G., Gloeckler, G.: Energetic particles in the vicinity of a possible neutral line in the plasma sheet. J. Geophys. Res. **88**(A10), 7742–7752 (1983). doi:10.1029/JA088iA10p07742

Malmberg, J.H., Wharton, C.B.: Collisionless damping of electrostatic plasma waves. Phys. Rev. Lett. **13**(6), 184–186 (1964). doi:10.1103/PhysRevLett.13.184

Matsumoto, H., Kojima, H., Miyatake, T., Omura, Y., Okada, M., Nagano, I., Tsutsui, M.: Electrostatic solitary waves (ESW) in the magnetotail: BEN wave forms observed by GEOTAIL. Geophys. Res. Lett. **21**(25), 2915–2918 (1994). doi:10.1029/94gl01284

Matthaeus, W.H., Ambrosiano, J.J., Goldstein, M.L.: Particle acceleration by turbulent magnetohydrodynamic reconnection. Phys. Rev. Lett. **53**(15), 1449–1452 (1984). doi:10.1103/PhysRevLett.53.1449

Ng, C.S., Bhattacharjee, A., Skiff, F.: Weakly collisional Landau damping and three-dimensional Bernstein-Greene-Kruskal modes: new results on old problems. Phys. Plasmas **13**(5), 055903–055909 (2006). doi:10.1063/1.2186187

Øieroset, M., Lin, R.P., Phan, T.D., Larson, D.E., Bale, S.D.: Evidence for electron acceleration up to $\sim$ 300 kev in the magnetic reconnection diffusion region of Earth's magnetotail. Phys. Rev. Lett. **89**(19), 195001 (2002). doi:10.1103/PhysRevLett.89.195001

Øieroset, M., Phan, T.D., Fujimoto, M., Lin, R.P., Lepping, R.P.: In situ detection of collisionless reconnection in the Earth's magnetotail. Nature **412**(6845), 414–417 (2001). doi:10.1038/35086520

Oka, M., Fujimoto, M., Shinohara, I., Phan, T.D.: "Island surfing" mechanism of electron acceleration during magnetic reconnection. J. Geophys. Res. **115**(A8), A08223 (2010a). doi:10.1029/2010ja015392

Oka, M., Phan, T.-D., Krucker, S., Fujimoto, M., Shinohara, I.: Electron acceleration by multi-island coalescence. Astrophys. J. **714**(1), 915 (2010b). doi:10.1088/0004-637X/714/1/915

Omura, Y., Kojima, H., Matsumoto, H.: Computer simulation of electrostatic solitary waves: a nonlinear model of broadband electrostatic noise. Geophys. Res. Lett. **21**(25), 2923–2926 (1994). doi:10.1029/94gl01605

Parker, E.N.: Sweet's mechanism for merging magnetic fields in conducting fluids. J. Geophys. Res. **62**(4), 509–520 (1957). doi:10.1029/JZ062i004p00509

Petschek, H.E.: Magnetic field annihilation. In: Hess, W.N. (ed.) AAS/NASA Symposium on the Physics of Solar Flares, pp. 425–439. NASA SP-50, Washington, DC (1964)

Phan, T.D., Gosling, J.T., Davis, M.S., Skoug, R.M., Oieroset, M., Lin, R.P., Lepping, R.P., McComas, D.J., Smith, C.W., Reme, H., Balogh, A.: A magnetic reconnection X-line extending more than 390 Earth radii in the solar wind. Nature **439**(7073), 175–178 (2006). doi:10.1038/nature04393

Pritchett, P.L.: Relativistic electron production during driven magnetic reconnection. Geophys. Res. Lett. **33**(13), L13104 (2006a). doi:10.1029/2005gl025267

Pritchett, P.L.: Relativistic electron production during guide field magnetic reconnection. J. Geophys. Res. **111**(A10), A10212 (2006b). doi:10.1029/2006ja011793

Pritchett, P.L.: Energetic electron acceleration during multi-island coalescence. Phys. Plasmas **15**(10), 102105–102109 (2008). doi:10.1063/1.2996321

Samtaney, R., Loureiro, N.F., Uzdensky, D.A., Schekochihin, A.A., Cowley, S.C.: Formation of plasmoid chains in magnetic reconnection. Phys. Rev. Lett. **103**(10), 105004 (2009). doi:10.1103/PhysRevLett.103.105004

Sweet, P.A.: The neutral point theory of solar flares. In: Lehnert, B. (ed.) Electromagnetic Phenomena in Cosmical Physics, pp. 123–134. Cambridge University Press, Cambridge (1958)

Uzdensky, D.A., Kulsrud, R.M.: Two-dimensional numerical simulation of the resistive reconnection layer. Phys. Plasmas **7**(10), 4018–4030 (2000). doi:10.1063/1.1308081

Wang, Y., Wei, F.S., Feng, X.S., Zhang, S.H., Zuo, P.B., Sun, T.R.: Energetic electrons associated with magnetic reconnection in the magnetic cloud boundary layer. Phys. Rev. Lett. **105**(19), 195007 (2010). doi:10.1103/PhysRevLett.105.195007

Wang, Y., Wei, F.S., Feng, X.S., Zuo, P.B., Guo, J.P., Xu, X.J., Li, Z.: Variations of solar electron and proton flux in magnetic cloud boundary layers and comparisons with those across the shocks and in the reconnection exhausts. Astrophys. J. **749**(1), 82 (2012). doi:10.1088/0004-637X/749/1/82

Wei, F.S., Feng, X., Yang, F., Zhong, D.: A new non-pressure-balanced structure in interplanetary space: Boundary layers of magnetic clouds. J. Geophys. Res. **111**(A3), A03102 (2006). doi:10.1029/2005ja011272

Wei, F.S., Hu, Q., Feng, X., Fan, Q.: Magnetic reconnection phenomena in interplanetary space. Space Sci. Rev. **107**(1), 107–110 (2003a). doi:10.1023/a:1025563420343

Wei, F.S., Liu, R., Fan, Q., Feng, X.: Identification of the magnetic cloud boundary layers. J. Geophys. Res. **108**(A6), 1263 (2003b). doi:10.1029/2002ja009511

Wei, F.S., Liu, R., Feng, X., Zhong, D., Yang, F.: Magnetic structures inside boundary layers of magnetic clouds. Geophys. Res. Lett. **30**(24), 2283 (2003c). doi:10.1029/2003gl018116

Wei, F.S., Zhong, D., Feng, X., Yang, F.: WIND observations of plasma waves inside the magnetic cloud boundary layers. Chin. Sci. Bull. **50**(17), 1906–1911 (2005). doi:10.1360/982004-577

Wilson III, L.B., Cattell, C., Kellogg, P.J., Goetz, K., Kersten, K., Hanson, L., MacGregor, R., Kasper, J.C.: Waves in interplanetary shocks: a WIND/WAVES study. Phys. Rev. Lett. **99**(4), 041101 (2007). doi:10.1103/PhysRevLett.99.041101

Xu, X., Wei, F., Feng, X.: Observations of reconnection exhausts associated with large-scale current sheets within a complex ICME at 1 AU. J. Geophys. Res. **116**(A5), A05105 (2011). doi:10.1029/2010ja016159

Zelenyi, L.M., Lominadze, J.G., Taktakishvili, A.L.: Generation of the energetic proton and electron bursts in planetary magnetotails. J. Geophys. Res. **95**(A4), 3883–3891 (1990). doi:10.1029/JA095iA04p03883

Chapter 2
Magnetic Reconnection and the Associated Energetic Particles in the Boundary Layer

2.1 Introduction

Previous studies have shown that BL is a turbulent layer formed by the interaction of the MC and the ambient solar wind (Wei et al. 2003a, b, c). Compared with those in the nearby upstream solar wind, the magnetic field in the BL is decreased and the plasma is compressed and heated. These features indicate that magnetic reconnection could prevail in the BL, but the 'direct evidence,' the Alfvénic reconnection jets, has not been found (Wei et al. 2006). In addition, although energetic electrons associated with magnetic reconnection in the solar flares and magnetotail have been reported (Imada et al. 2007; Lin and Hudson 1971; Øieroset et al. 2002), no such energetic electrons have so far been found in the solar wind reconnection. After analyzing 7 reconnection exhausts observed by ACE spacecraft (Fig. 2.1), Gosling et al. (2005a) found that no evidence for any substantial increase in energetic particle intensity associated with these events. So they suggest that local reconnection is not a significant source of energetic particles in the solar wind and reconnection itself may not be a particularly effective process for populating other space and astrophysical environments with energetic particles (Gosling et al. 2005a).

In this chapter, we report a Petschek-like reconnection with roughly Alfvénic reconnection jets inside a BL and present the first observation of energetic particles accelerated by magnetic reconnection in the solar wind.

2.2 Analyzing Methods

Compared with the magnetic reconnection in the magnetotail, where the reconnection X-line and reconnection jets generally point to the Z and X directions in geocentric solar ecliptic (GSE) coordinate (Fig. 1.7), in most cases, it is not very easy to discriminate the reconnection in the solar wind from the unambiguous

© Springer-Verlag Berlin Heidelberg 2016

Y. Wang, *Magnetic Cloud Boundary Layers and Magnetic Reconnection*,
Springer Theses, DOI 10.1007/978-3-662-48310-7_2

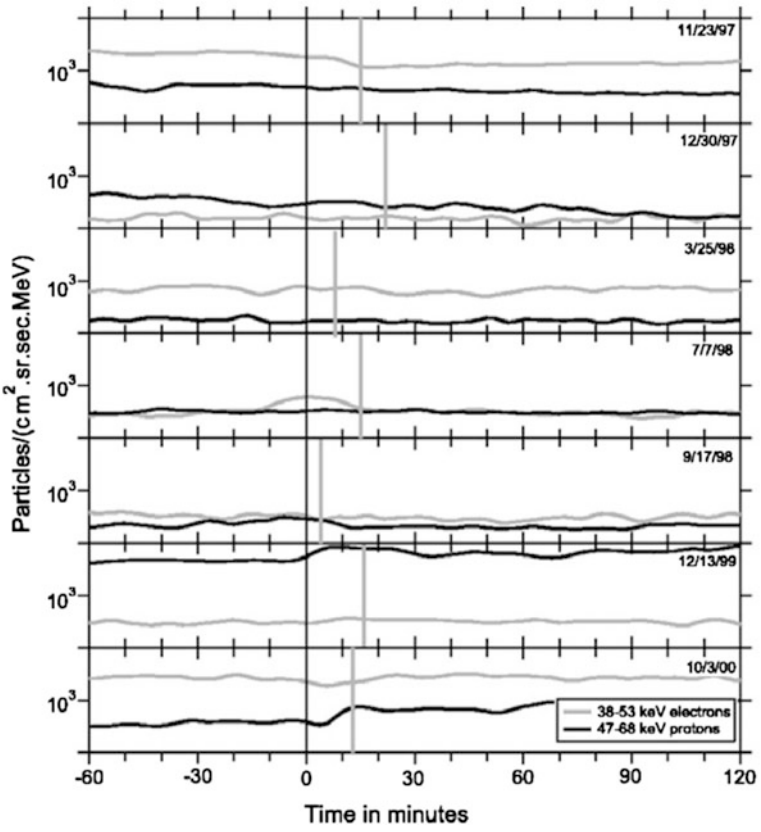

Fig. 2.1 Ion and electron fluxes observed by ACE spacecraft. The beginning of exhausts are shifted to t = 0 (*black vertical line*) and the end of the exhausts are marked by *gray vertical line*. Reproduced from (Gosling et al. 2005a), by permission of John Wiley and Sons Ltd

signatures in GSE coordinates. So it is necessary to construct a new coordinate based on the reconnection current sheet.

2.2.1 LMN Coordinate

To facilitate analyzing magnetic reconnection, we try to constructed the LMN coordinate (Hudson 1970; Sonnerup and Cahill 1967) based on the reconnection current sheet (Fig. 2.2). In this coordinate, L points along the antiparallel magnetic field direction, N points along the overall current sheet normal and M points along the X-line direction. Practically, each direction could be deduced by the minimum variance analysis of magnetic field (MVAB) (Paschmann and Daly 1998).

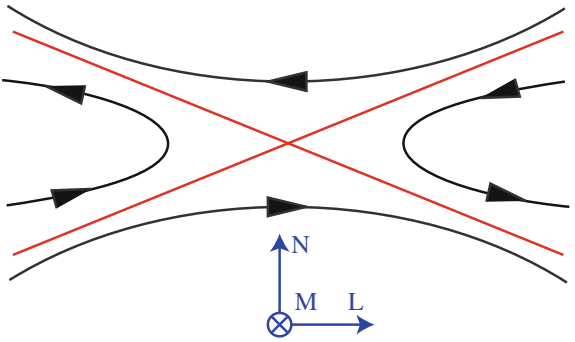

Fig. 2.2 Magnetic reconnection shown in LMN coordinate

2.2.2 Walen Relation

When a spacecraft crosses a reconnection exhaust, the Alfvénic reconnection jets could be described by the Walen relation in the form of:

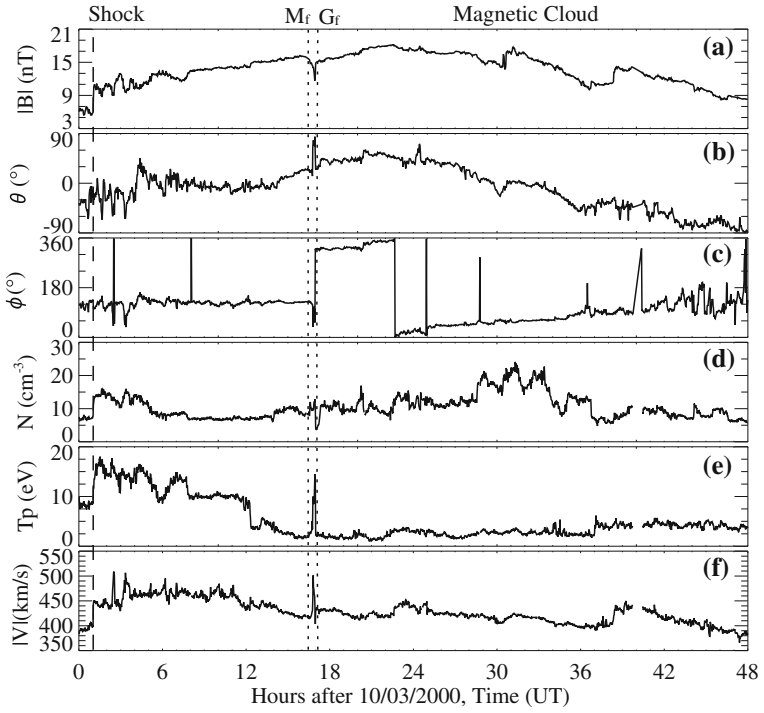

Fig. 2.3 **a–f** WIND measurements of the magnetic field strength, latitude angle, azimuth angle, proton density, temperature, and velocity. The *left dashed line* shows a shock driven by the MC. The BL is bounded by the *dot lines* (marked by Mf and Gf)

$$\mathbf{V}_{pre} = \mathbf{V}_{ref} \pm \sqrt{\frac{\rho_{ref}(1-\alpha_{ref})}{\mu_0}}\left(\frac{\mathbf{B}}{\rho} - \frac{\mathbf{B}_{ref}}{\rho_{ref}}\right). \tag{2.1}$$

Here ρ, V, and B represent plasma density, velocity vector, and magnetic field vector, while $\alpha=(p_{//}-p_{\perp})\mu_0/B^2$ is the pressure anisotropy factor. The subscript 'ref' denotes the reference time at the leading (trailing) edge of the exhaust and 'pre' denotes the calculated velocity across the region. The positive (negative) sign is chosen for the trailing (leading) edge of the exhaust.

2.3 Magnetic Reconnection in the BL

Figure 2.3 provides an overview of solar wind conditions measured at (32.6, −251.7, −3.8)Re in GSE coordinate on 3rd October 2000 by the Wind spacecraft. The MC's leading edge, marked between Mf and Gf, reveals a decreased field

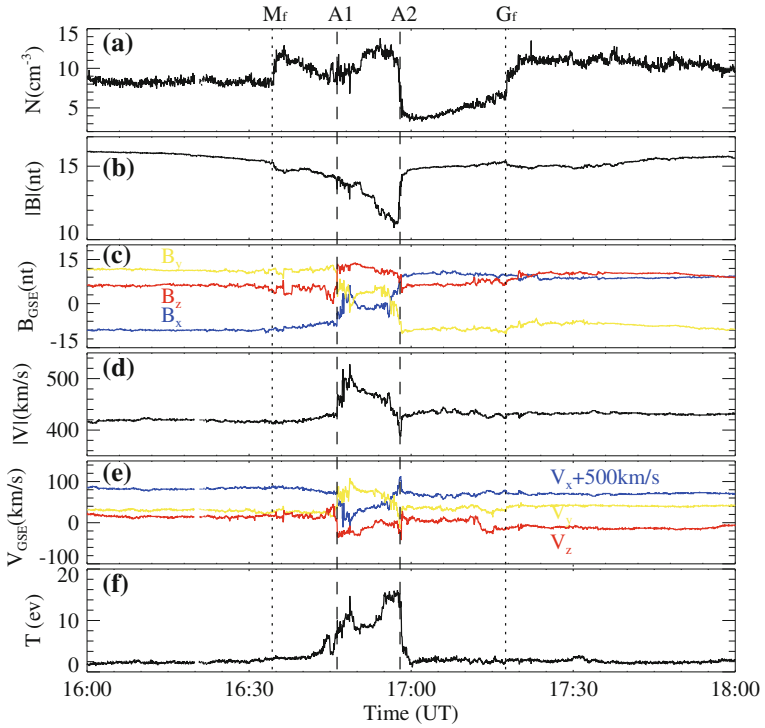

Fig. 2.4 **a–f** WIND measurements of density, magnetic field, velocity (Vx has been shifted by 500 km/s), and temperature between 16:00 and 18:00 UT on October 3, 2000 with a cadence of 3 s. The MCBL is shown by the *dotted lines*; the *dashed lines* marked by A1 and A2 inside the BL represent the reconnection exhaust boundaries at 16:46 UT and 16:58 UT, respectively. Reprinted with permission from (Wang et al. 2010), Copyright 2010 by American Physical Society

strength, sudden change in field orientations, increased flow velocity and proton temperature.

Figure 2.4 shows more detailed information between 16:00 and 18:00 UT. According to further analysis, it is found that the area between 16:46 and 16:58 UT (marked by A1 and A2) exhibits the general characteristics of magnetic reconnection. In particular, the magnetic field in the X and Y directions are almost reversed, and the total magnitude of magnetic field declines $\sim$4nT and rotates $\sim$143°. Moreover, the plasma velocity increases $\sim$100 km/s and the proton temperature increases $\sim$10 eV. All these features indicate that WIND spacecraft may encounter a reconnection exhaust.

To see the reconnection exhaust more clearly, the LMN current sheet coordinate system is constructed and shown in Fig. 2.5. The current sheet normal N, (0.76, 0.64, 0.06) in GSE, is calculated by minimum variance analysis of the magnetic field (MVAB) across the exhaust (Paschmann and Daly 1998). So is the X-line direction M, (−0.02, −0.06, 0.99) in GSE, nearly perpendicular to the ecliptic plane. We assume that the associated MC has a flux-rope-like structure (Burlaga 1995) and get its axis pointing to (−0.84, 0.23, 0.49) in GSE. Figure 2.3a reconstructs the geometric configuration of the reconnection event.

Fortunately, this reconnection exhaust is also observed by the ACE spacecraft located at (255.2, −29.2, −7.5)Re. Since ACE is farther away from the X-line than WIND, it takes ACE 14 min, which is 2 min longer than Wind, to cross the exhaust. Detailed magnetic field and velocity conditions projected in the LMN coordinate

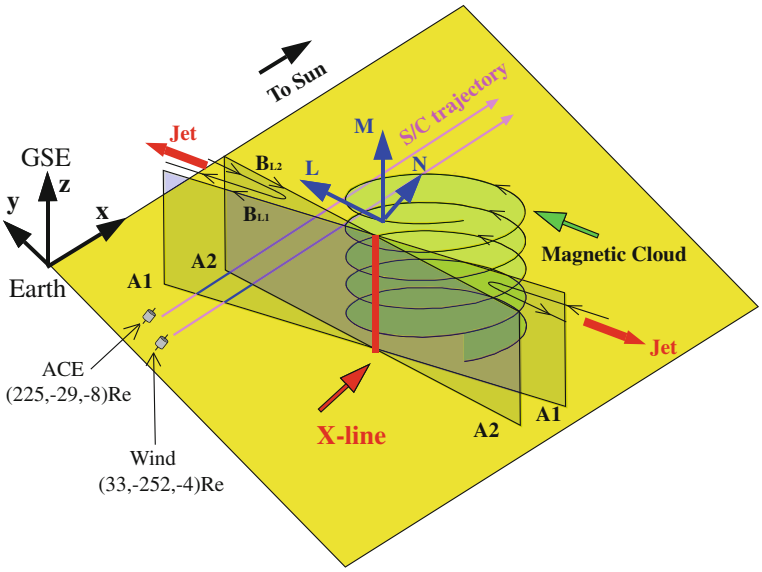

Fig. 2.5 Geometric configuration of the reconnection exhaust; the reconnection jets and X lines are shown in *red*; the following MC is sketched in *green*. Reprinted with permission from (Wang et al. 2010), Copyright 2010 by American Physical Society

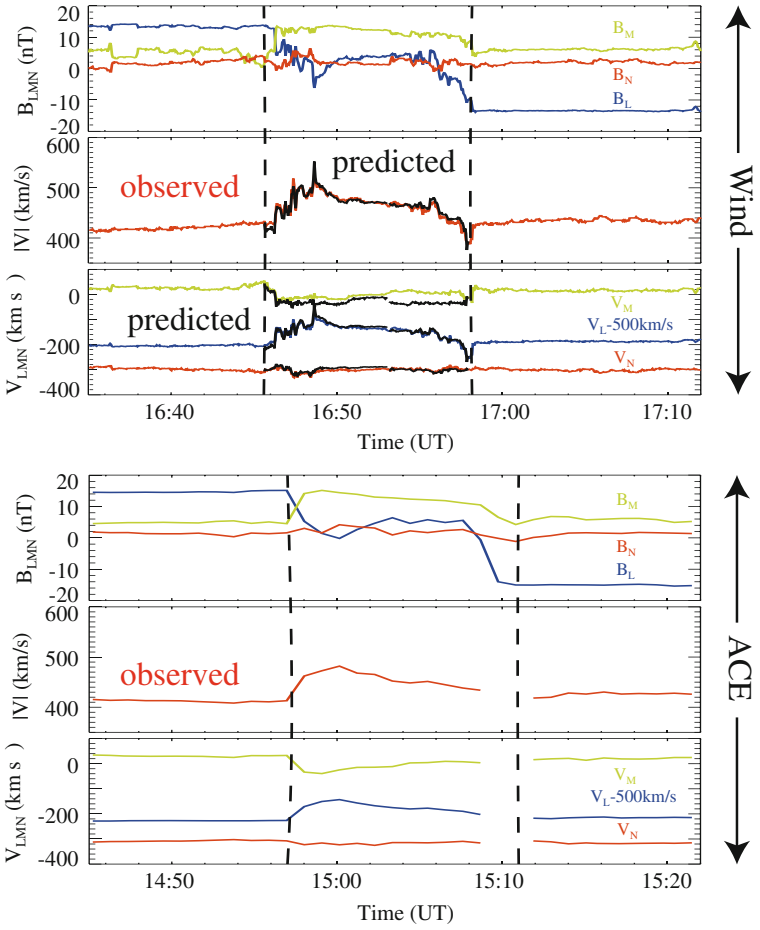

Fig. 2.6 measurements of magnetic field and velocity in the LMN coordinate system (V_L has been shifted by −500 km/s). The *dashed lines* denote the exhaust boundaries and the *black lines* stand for the reconnection jets calculated by Walen relation. The pressure anisotropy factor is set to zero in this calculation

are shown in Fig. 2.6. It could be found that the normal magnetic field B_N is almost constant and near zero, while the antiparallel magnetic field B_L component changes from +14 nT to −14 nT, entirely reversed all over the exhaust. In addition, V_N is roughly steady while V_L increases $\sim$100 km/s in the exhaust. Moreover, we use WIND data[1] to compare the observed plasma velocity in the exhaust with the prediction given by Walen relation (Eq. 2.1). As seen in Fig. 2.6, both magnitude

[1]The data provided by the ACE spacecraft is not used to calculate the predicated velocity since there is a data gap near the trailing edge of the exhaust.

and components of the predicted velocity agree well with the observations. The increased velocity is mainly in the L direction and the increment is close to the Alfvén speed. The observed plasma flows exhibit primary features of reconnection jets. All these evidences indicate that WIND and ACE spacecraft detected a reconnection exhaust in the BL.

2.4 Energetic Particles Associated with Magnetic Reconnection

In this event, we fortunately observed energetic particles associated with magnetic reconnection that has not been so far reported in the solar wind. As shown in Fig. 2.7, the increments of particle fluxes display strong energy selectivity and pitch angle dependency. Particularly, (1) low-energy electrons were mainly heated

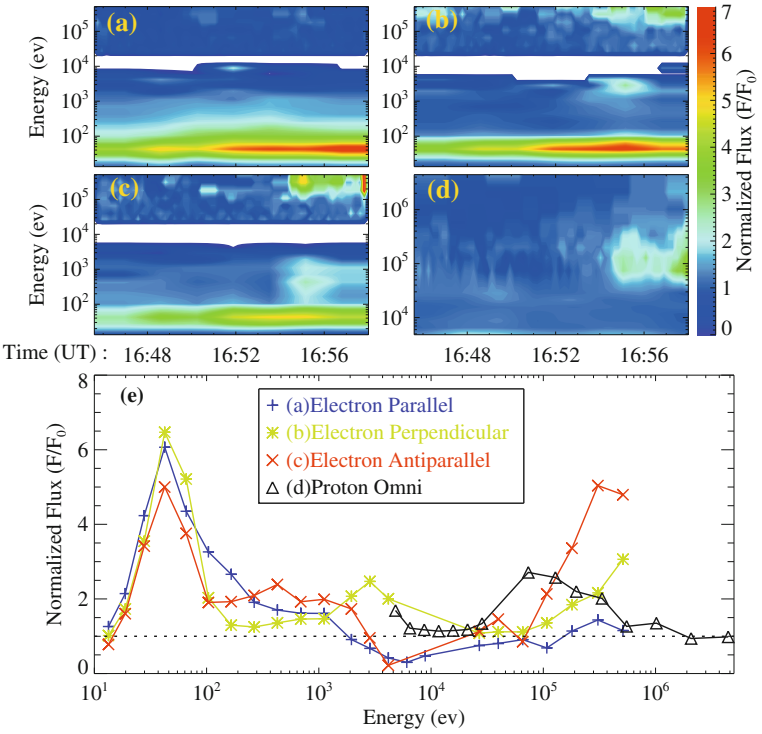

Fig. 2.7 Wind measurements of 10 eV–500 keV electrons normalized fluxes in parallel (**a**), perpendicular (**b**) and antiparallel (**c**) directions, respectively. **d** 5–5000 keV protons normalized omni flux. All the fluxes are divided by the mean background flux F0 at every energy band for normalizing. The background flux F0 is chosen by the mean flux of a nearby quiet period (between 16:00 and 16:3 UT) for each energy band. The missing data is shown by blank. **e** Combined normalized fluxes at 16:55 UT for a typical show. Reprinted with permission from (Wang et al. 2010), Copyright 2010 by American Physical Society

around 10–200 eV with an intense enhancement near 50 eV which resembles the observations of Huttunen (Huttunen et al. 2008). (2) 1–100 keV electrons do not show such enhancement, while 100–500 keV electron fluxes mainly increase at pitch angle between 90 and 180° (perpendicular and antiparallel to the field line). (3) The protons are accelerated around 100 keV, but no remarkable increments are found in other energy bands.

In the high-energy range (100–500 keV) where our greatest concern exists, the electron has a burst increase near 16:55 UT. As shown in Fig. 2.8, the least square fits of the electrons and protons, measured by WIND (SST-Foil), also show power law distributions ($f(v) \propto E^{-k}$) with a smaller power index k inside the exhaust and larger ones outside. Although the spacecraft does not cross the reconnection diffusion region, where the energetic electrons were thought to be initially produced, we can still rule out the possibility that such irregular flux enhancements are merely

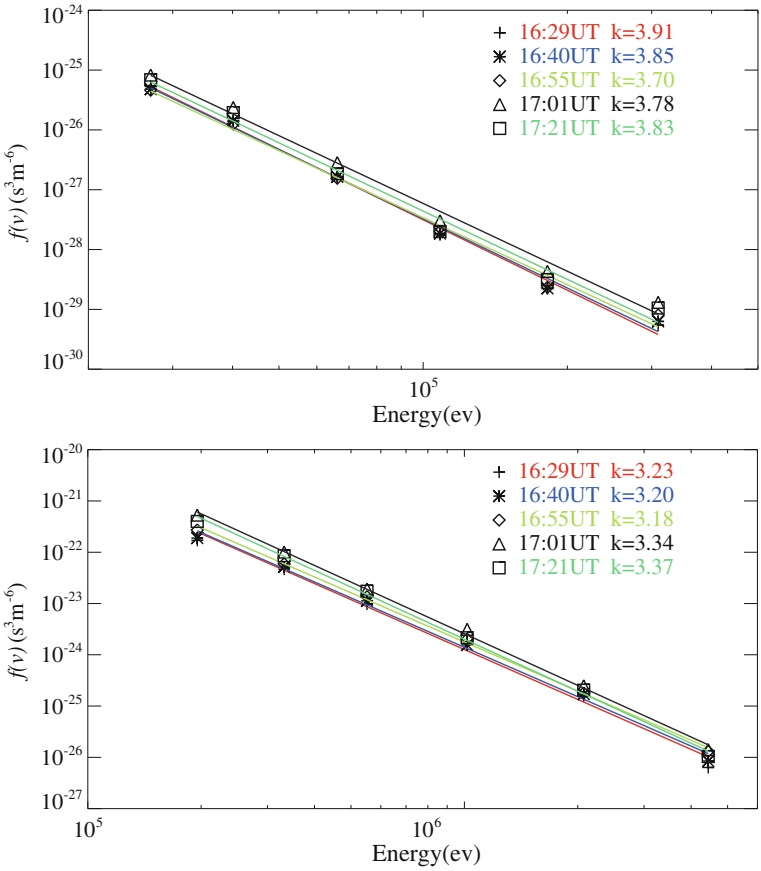

Fig. 2.8 Energy spectrum of electron (*up*) and proton (*down*) fitted by a power law distribution near the reconnection exhaust

caused by the variation of background electron temperature or density (see the isotropic low-energy electrons around 40 eV for example). Instead, both the reconnection topological structure and the harder spectrum in the exhaust suggest that they are most probably accelerated by magnetic reconnection and then expelled through the long reconnection separatrices (Egedal et al. 2009; Pritchett 2006). Since the local magnetic field at 16:55 UT just points to the reconnection region and the expelled energetic electrons are mainly concentrated near the specified two of the four reconnection separatrices by the modulation of the guide field (Egedal et al. 2009; Pritchett 2006), the Wind spacecraft would naturally measure enhanced field-aligned energetic electrons in the antiparallel direction (Fig. 2.7).

2.5 Discussion and Conclusion

The small normal velocity shear (ΔV_N = 12 km/s) across bifurcated current sheet could be considered as a V_{in} = 6 km/s reconnection inflow. Correspondingly, the reconnection electric field is calculated to be E = 0.084 mV/m ($E = B \times V_{in}$) and the dimensionless reconnection rate could be estimated by V_{in}/V_A = 5.3 % (V_A = 113 km/s is the external Alfvén speed). These signatures are consistent with the Petschek-like model of fast reconnection and they also resemble the previous observations.

In this event, it takes ACE spacecraft 14 min to cross the exhaust with a 300 km/s velocity (V_N). So the width of the exhaust could be calculated to be $\sim 2.5 \times 10^5$ km (or 40 Re) and the distance to the X-line is $\sim 2.4 \times 10^6$ km (or 374 Re). The observational location of ACE is so far away from the X-line ($\sim 32308 d_i$), and no hall signatures are observed in this area.

Nevertheless, it is difficult to calculate the real length of the X-line since its direction (M) is nearly perpendicular to the ecliptic plane (M = [−0.02nx, −0.06ny, 0.99nz] in GSE), while both spacecrafts are almost in that plane. However, the observed similar characteristics make it reasonable to believe that this Petschek-like reconnection with quasi-steady and large-scale properties also has a long reconnection X-line extending several hundreds of earth radius as those previously reported observations (Gosling et al. 2007; Phan et al. 2006). If the X-line could extend to $\sim$668 Re as is observed in previous event (Gosling et al. 2007), the reconnection potential energy is $\sim$358 keV, and this energy might play an important role in the acceleration of energetic particles.

To sum up, we observed a magnetic reconnection exhaust in a BL. After the detailed analyses, it is found that the reconnection jets meet the Walen relation, and this event belongs to Petschek-like fast reconnection which has large-scale and quasi-steady properties as previous observations (Davis et al. 2006; Gosling 2011; Gosling et al. 2005b, 2007; Phan et al. 2006). In addition, the first observation of energetic particles (100–500 keV electrons and $\sim$100 keV protons) associated with magnetic reconnection in the solar wind is reported.

References

Burlaga, L.F.: Interplanetary Magnetohydrodynamics. Oxford Univ. Press, New York (1995)

Davis, M.S., Phan, T.D., Gosling, J.T., Skoug, R.M.: Detection of oppositely directed reconnection jets in a solar wind current sheet. Geophys. Res. Lett. **33**(19), L19102 (2006). doi:10.1029/2006gl026735

Egedal, J., Daughton, W., Drake, J.F., Katz, N., Le, A.: Formation of a localized acceleration potential during magnetic reconnection with a guide field. Phys. Plasmas **16**(5), 050701–050704 (2009). doi:10.1063/1.3130732

Gosling, J.T.: Magnetic reconnection in the solar wind. Space Sci. Rev. 1–14 (2011). doi:10.1007/s11214-011-9747-2

Gosling, J.T., Eriksson, S., Blush, L.M., Phan, T.D., Luhmann, J.G., McComas, D.J., Skoug, R. M., Acuna, M.H., Russell, C.T., Simunac, K.D.: Five spacecraft observations of oppositely directed exhaust jets from a magnetic reconnection X-line extending > 4.26×10^6 km in the solar wind at 1 AU. Geophys. Res. Lett. **34**(20), L20108 (2007). doi:10.1029/2007gl031492

Gosling, J.T., Skoug, R.M., Haggerty, D.K., McComas, D.J.: Absence of energetic particle effects associated with magnetic reconnection exhausts in the solar wind. Geophys. Res. Lett. **32**(14), L14113 (2005a). doi:10.1029/2005gl023357

Gosling, J.T., Skoug, R.M., McComas, D.J., Smith, C.W.: Direct evidence for magnetic reconnection in the solar wind near 1 AU. J. Geophys. Res. **110**(A1), A01107 (2005b). doi:10.1029/2004ja010809

Hudson, P.D.: Discontinuities in an anisotropic plasma and their identification in the solar wind. Planet. Space Sci. **18**(11), 1611–1622 (1970). doi:10.1016/0032-0633(70)90036-x

Huttunen, K.E.J., Bale, S.D., Salem, C.: Wind observations of low energy particles within a solar wind reconnection region. Ann Geophys-Germany **26**(9), 2701–2710 (2008). doi:10.5194/angeo-26-2701-2008

Imada, S., Nakamura, R., Daly, P.W., Hoshino, M., Baumjohann, W., Mühlbachler, S., Balogh, A., Rème, H.: Energetic electron acceleration in the downstream reconnection outflow region. J. Geophys. Res. **112**(A3), A03202 (2007). doi:10.1029/2006ja011847

Lin, R.P., Hudson, H.S.: 10–100 keV electron acceleration and emission from solar flares. Sol. Phys. **17**(2), 412–435 (1971). doi:10.1007/bf00150045

Øieroset, M., Lin, R.P., Phan, T.D., Larson, D.E., Bale, S.D.: Evidence for electron acceleration up to $\sim$ 300 keV in the magnetic reconnection diffusion region of Earth's magnetotail. Phys. Rev. Lett. **89**(19), 195001 (2002). doi:10.1103/PhysRevLett.89.195001

Paschmann, G., Daly, P.W.: Analysis Methods for Multi-Spacecraft Data. ESA Publications Division, Bern (1998)

Phan, T.D., Gosling, J.T., Davis, M.S., Skoug, R.M., Oieroset, M., Lin, R.P., Lepping, R.P., McComas, D.J., Smith, C.W., Reme, H., Balogh, A.: A magnetic reconnection X-line extending more than 390 Earth radii in the solar wind. Nature **439**(7073), 175–178 (2006). doi:10.1038/nature04393

Pritchett, P.L.: Relativistic electron production during guide field magnetic reconnection. J. Geophys. Res. **111**(A10), A10212 (2006). doi:10.1029/2006ja011793

Sonnerup, B.U.Ö., Cahill Jr, L.J.: Magnetopause structure and attitude from explorer 12 observations. J. Geophys. Res. **72**(1), 171–183 (1967). doi:10.1029/JZ072i001p00171

Wang, Y., Wei, F.S., Feng, X.S., Zhang, S.H., Zuo, P.B., Sun, T.R.: Energetic electrons associated with magnetic reconnection in the magnetic cloud boundary layer. Phys. Rev. Lett. **105**(19), 195007 (2010). doi:10.1103/PhysRevLett.105.195007

Wei, F.S., Feng, X., Yang, F., Zhong, D.: A new non-pressure-balanced structure in interplanetary space: boundary layers of magnetic clouds. J. Geophys. Res. **111**(A3), A03102 (2006). doi:10.1029/2005ja011272

Wei, F.S., Hu, Q., Feng, X., Fan, Q.: Magnetic reconnection phenomena in interplanetary space. Space Sci. Rev. **107**(1), 107–110 (2003a). doi:10.1023/a:1025563420343

Wei, F.S., Liu, R., Fan, Q., Feng, X.: Identification of the magnetic cloud boundary layers. J. Geophys. Res. **108**(A6), 1263 (2003b). doi:10.1029/2002ja009511

Wei, F.S., Liu, R., Feng, X., Zhong, D., Yang, F.: Magnetic structures inside boundary layers of magnetic clouds. Geophys. Res. Lett. **30**(24), 2283 (2003c). doi:10.1029/2003gl018116

Chapter 3
The Acceleration of Energetic Particles in Magnetic Reconnection

3.1 Introduction

Magnetic reconnection acts as an efficient accelerator to generate energetic particles that could be found in the solar corona, solar wind, and magnetotail. Up to now, it is not clear that how the energetic particles are accelerated to hundreds of kiloelectronvolt (keV) or even higher energy during the reconnection process. In the past few decades, many authors have used numerical simulations to investigate the acceleration of energetic particles in magnetic reconnection and built remarkable acceleration models (Ambrosiano et al. 1988; Birn et al. 2000, 2004; Blackman and Field 1994; Dmitruk et al. 2004; Drake et al. 2003, 2006; Goldstein et al. 1986; Hoshino 2005, 2012; Hoshino et al. 2001; Imada et al. 2007; Matthaeus et al. 1984; Oka et al. 2010a, b; Pritchett 2006a, b, 2008; Speiser 1965). However, as discussed in the previous chapter, these acceleration models have some limitations, especially when they are applied to the large-scale magnetic reconnection exhaust in solar wind. Thus, it is important to know why these energetic particles are missed in these reconnection events and how they are produced.

In this chapter, we will discuss the energetic electron acceleration problem in large-scale reconnection exhaust under real solar wind conditions by numerical simulations. First, we set up a MHD simulation for the reconnection event driven by MC on October 3, 2000, to reveal its global evolution. Then we carry out another MHD computation using initial conditions similar to the geospace environmental modeling (GEM) reconnection challenge (Birn et al. 2001) and get the background time-varying magnetic field and electric field, and finally, the test particle approach is applied to trace the details of the electron energization (Wang et al. 2010).

The reconnection exhaust can extend up to $\sim 10^7$ km (Lavraud et al. 2009), (e.g. Fig. 3.1), while the depth of the reconnection current sheet is of the order of ion inertial length ($\sim 10^2$ km). Due to the scale difference, it is difficult to carry out a global simulation that can both reveal the macroscopic evolutions of the reconnection event and resolve the microscopic dynamics in the reconnection diffusion

© Springer-Verlag Berlin Heidelberg 2016

Y. Wang, *Magnetic Cloud Boundary Layers and Magnetic Reconnection*,
Springer Theses, DOI 10.1007/978-3-662-48310-7_3

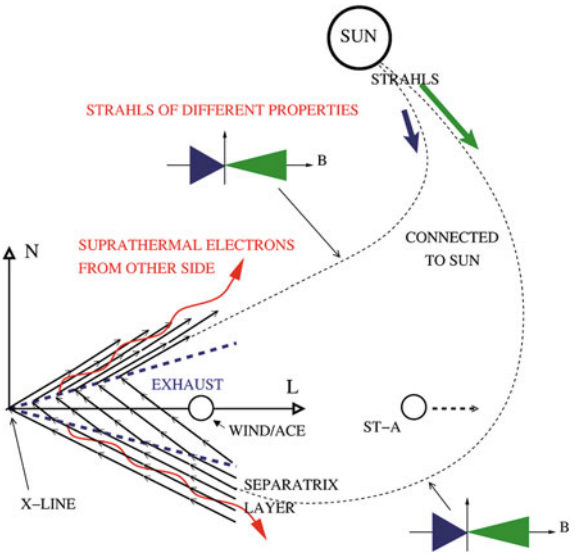

Fig. 3.1 A complex reconnection exhaust extends over 1800Re. Reprinted from (Lavraud et al. 2009), with kind permission from Springer Science + Business Media

region. Therefore, we use the adaptive mesh refinement (AMR) technique to handle the MHD simulations (Zhang et al. 2011).

3.2 Background Description of Numerical Simulations

3.2.1 Different Methods of Numerical Simulations

Test particle approach is a useful tool to discuss the particle acceleration problem. It ignores interactions between different particles. The electric field and magnetic field introduced by the charged particles are also ignored. This method can be used in tenuous plasma environment and many authors have used it to trace the particle trajectories inside the current sheet in the early times (Sonnerup 1971; Speiser 1965). The basic idea of test particle approach is to solve the Lorentz equations as written below:

$$\begin{cases} \dfrac{dP}{dt} = q(E + v \times B) \\ \dfrac{dR}{dt} = v \\ P = \gamma m v \\ \gamma = \dfrac{1}{\sqrt{1 - \frac{v^2}{c^2}}} \end{cases}$$

where *P, E, v, B, and R* are momentum, electric field, velocity, magnetic field, and position vector; m is the mass of a particle, q is the electric charge, and c is the speed of light in vacuum. This method can provide a good approximation for physical phenomena and since it simplifies the problems, it costs relatively little time to finish the computation. Even now, it is still a powerful tool to diagnose the acceleration problem of energetic particles (Birn et al. 2004; Dmitruk et al. 2004).

Unlike the test particle simulation, particle in cell (PIC) simulation has a distinct feature. It calculates the electric field and magnetic field introduced by each particle on fixed meshes. In such a framework, both wave-particle interactions and particle −particle interactions can be revealed. In addition, PIC simulation is more self-consistent than test particle simulation. However, it requires a lot of computational resources, and it becomes impossible to set up a PIC simulation when the computational domain increases to a certain large scale.

MHD simulation, which is widely used in space plasma physics, treats particles as a whole, and puts emphasis on their bulk movements. In MHD simulations, the velocity of particles in magnetic reconnection is of the order of Alfvén speed (Liu et al. 2009). Obviously, such velocity is too slow in the realm of energetic particle acceleration. However, MHD simulation can provide electric field and magnetic field (Fig. 3.2) that are needed by further analyses of particle acceleration such as the computations in test particle simulation.

3.2.2 GEM Magnetic Reconnection Challenge

The MHD simulation of magnetic reconnection used in this chapter is similar to the GME reconnection challenge with a guide field (Birn et al. 2001). The initial configuration is based on the generalized 2-D Harris current sheet in xy plane with thickness 2λ. The magnetic field B and density n can be written as

$$B_x(y) = B_0 \tan h(y/\lambda)$$

$$n(y) = n_0 \mathrm{sech}^2(y/\lambda) + 0.2n_0$$

The pressure balance condition can be revealed by

$$n_0 k(T_e + T_p) = B_0^2/(2\mu_0).$$

The whole computation domain is $[-L_x/2 < x < L_x/2]$ and $[-L_y/2 < y < L_y/2]$ with periodic boundary conditions. To facilitate the magnetic reconnection, a small perturbation function ϕ in the center region $[x, y] = [0, 0]$ is added by

$$\phi(x, y) = \phi_0 \cos(2\pi x/L_x) \cos(2\pi y/L_y).$$

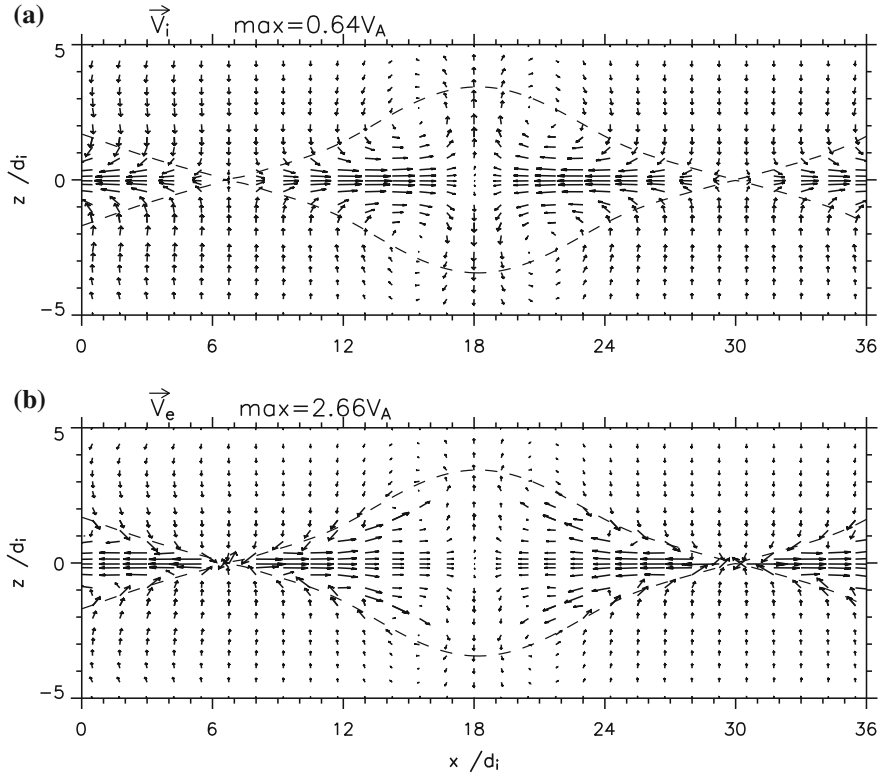

Fig. 3.2 Ion (*upper panel*) and electron (*lower panel*) flow fields in magnetic reconnection obtained from MHD simulation. Reproduced from (Liu et al. 2009), with permission of John Wiley and Sons Ltd

3.3 Simulation Results

3.3.1 Interplanetary Magnetic Reconnection Driven by MC

The evolution of magnetic reconnection depends much on the local environments, such as variations of plasma and magnetic field. First, we carry out MHD simulations to reveal the occurrence of magnetic reconnection driven by a MC in the solar wind. The model of the computation resembles those in our early calculations (Wei et al. 2003) and the initial conditions are taken from the real solar wind conditions on October 3, 2000. As seen from Figs. 3.3 and 3.4a, the MC can drive magnetic reconnection under certain local conditions. After the magnetic reconnection occurs, it continues with the propagation of the MC. In this ongoing process, magnetic reconnection forms large-scale reconnection exhaust whose length can even extend longer than the cross-section radius of the MC. These features are also consistent with the

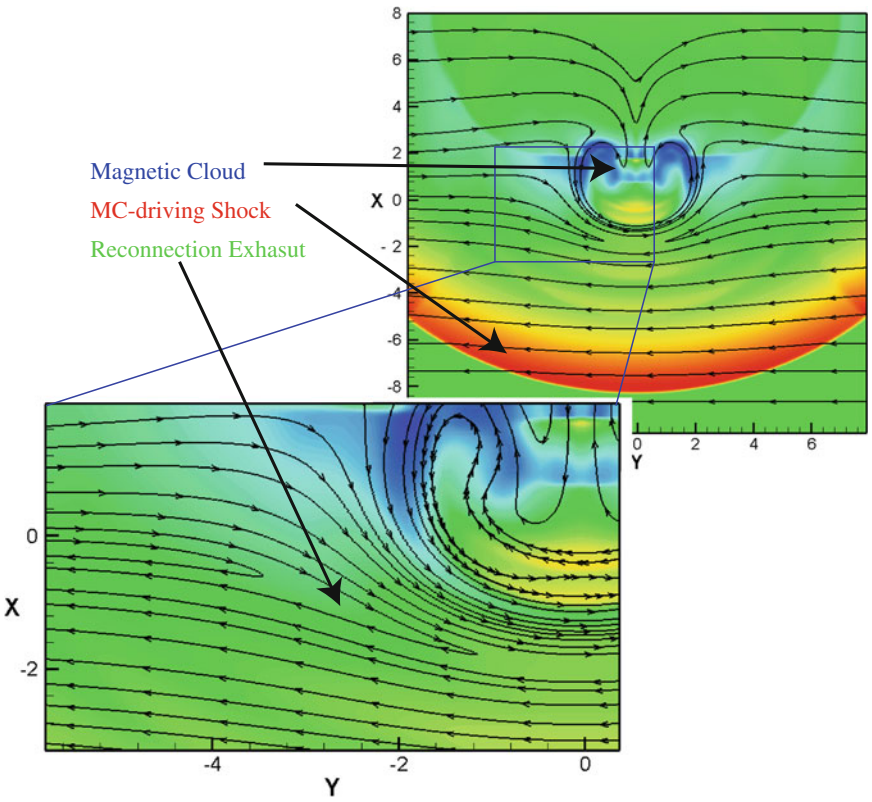

Fig. 3.3 MHD simulation results: the distribution of thermal pressure in the interplanetary magnetic reconnection driven by MC. Different colors represent different thermal pressure (*red* stronger; *blue* weaker). The *black lines* denote magnetic field lines. The *lower panel* is the zoomed view of the *blue square* in the *upper panel*

observations of large-scale and quasi-steady magnetic reconnection in the solar wind (Gosling 2011; Gosling et al. 2007, 2005; Phan et al. 2006).

3.3.2 Acceleration of Energetic Electrons

To reveal the details of the magnetic reconnection process, we carry out MHD simulations in the MC-driving reconnection center as seen in Fig. 3.4b. The model is similar to the GME reconnection challenge with a guide field, and the initial conditions are taken from the real solar wind. The guide field, the velocity of the vertically symmetrical driving flows, and the Lundquist number are set to 5nT, 6 km/s and 50,000, respectively. The aspect ratio of the Harris current sheet is set to 100, and the computation domain is $100d_i \times 10d_i$ ($d_i \sim 73$ km is the ion inertial length). Due to the

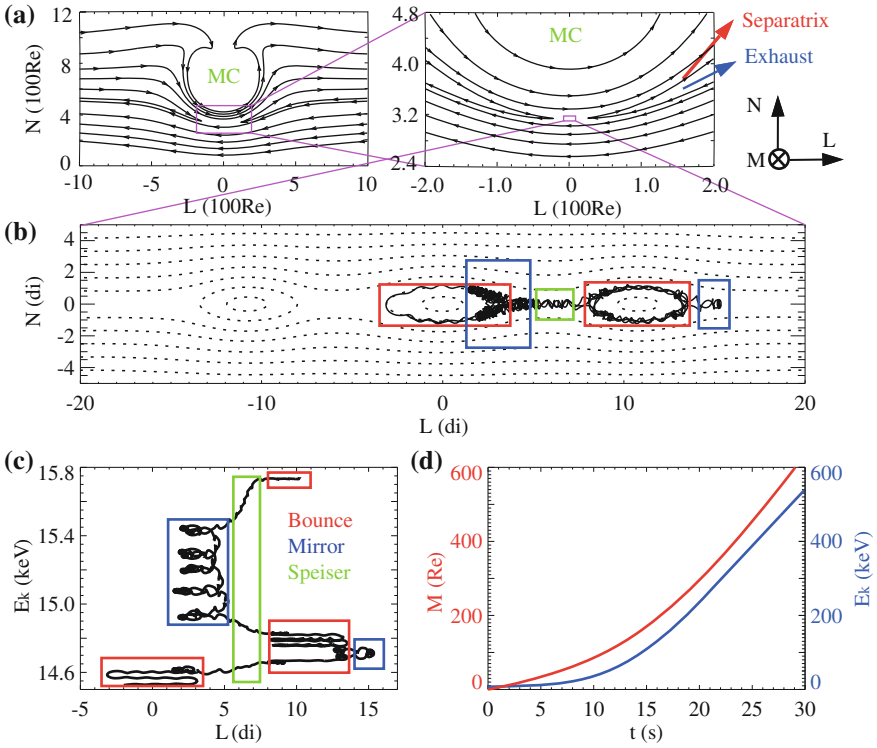

Fig. 3.4 **a** MHD parallel AMR simulation of the MC-driving magnetic reconnection in the solar wind (*left*) and the zoomed result (*right*). The magnetic field lines are sketched by the *solid lines*. **b** Simulation of magnetic reconnection in the reconnection center. The magnetic field lines are sketched by the *dotted lines*. **c** The electron energy E_k as a function of position in L direction in test particle simulation. Three typical motions are marked by colored *rectangles*. **d** The electron energy E_k (*blue*) and its M position (*red*) as a function of time during the whole acceleration process. Reprinted with permission from (Wang et al. 2010), Copyright 2010 by American Physical Society

squeezing of the driving flows together with the long current sheet (large aspect ratio), the guide field and the high Lundquist number conditions all prefer to generate magnetic island chain rather than form a single X-line in the reconnection center (Birn and Priest 2007; Drake et al. 2003, 2006; Pritchett 2006a, b). As discussed in the previous chapter, such configuration is conducive to electron acceleration. In addition, this large-scale reconnection usually has long-extend reconnection X-line, so that the electron can also get accelerated from the considerable reconnection potential energy.

We continue to run test particle simulations based on the calculated time-dependent electric field and magnetic field. We put a test electron in the reconnection region at [L, M, N] = [2.0, 0.0, 0.7]d_i to trace the typical acceleration processes. The initial kinetic energy of test electron is 14.4 keV and its pitch angel

is 10°. Figure 3.4b displays obviously three magnetic islands at $t = 151t_A$ (t_A is the Alfvén transit time, $1t_A = 0.53$ s).

It is seen from Fig. 3.4c that the test electron does not get accelerated all the time. Specifically, significant energizations mainly occur at three typical stages (marked by colored rectangles, respectively). At first, the electron bounces in the middle island in Fig. 3.4b and gets energy at the contracting island ends. In this stage, it gains energy from both the Fermi-type reflections and the electric field. Later, the electron crosses the current sheet to the right island and mirrors back in the magnetic field pileup region. In such Speiser-type and mirrored motions, it still gets accelerated by the electric field. Overall, the test electron switches among the three typical motions during the trapping status, and it gets energy from both the Fermi-type acceleration and the electric field until it totally drifts outside the reconnection region. In this simulation, it is demonstrated that even if the island contraction is throttled by the back pressure of the heated electrons and the large guide field, the electron can still get reconnection potential energy by drifting in the X-line direction. Finally, the electrons are accelerated to $\sim$500 keV in $\sim$30 s with a requirement of drifting $\sim$600 Re in the M direction (along the reconnection X-line).

3.4 Discussion and Summary

Compared with the long duration time of the reconnection process, the required time in the simulation is short, but it is enough for the acceleration. The $\sim$600 Re X-line is also acceptable in such Petschek-type reconnection. It is noteworthy that the final energy of the electron consists well with the observation. In addition, the energetic electrons will concentrate near the magnetic islands and current sheet in the simulation. Although this feature is not observed in this event since the spacecraft is far from the reconnection center, a similar phenomenon is also reported by other authors (Chen et al. 2008).

Traditional acceleration models can account for the acceleration of energetic electrons during the magnetic reconnection process under certain conditions (Ambrosiano et al. 1988; Birn et al. 2000, 2004; Blackman and Field 1994; Dmitruk et al. 2004; Drake et al. 2003, 2006; Goldstein et al. 1986; Hoshino 2005, 2012; Pritchett 2006b, 2008; Speiser 1965). However, there also exist limitations in these models. First, the single X-line configuration assumed by the electric field acceleration model may rarely exist under real solar wind conditions. In addition, the island's volume-filled structure required by the Fermi-type mechanism may also have difficulties in explaining why the expelled energetic electrons are always concentrated near the reconnection separatrices. More importantly, it may be also idealized for the referred models to treat acceleration of energetic electrons as a single mechanism-dominated process, especially in the solar wind.

Referring to this event again, it is almost impossible that the reconnection electric field itself can produce electrons up to 500 keV alone, because the

maximum reconnection potential energy is only 317 keV even if the X-line can extend as long as ~600Re in the simulation. On the other hand, the released energy from the contracting magnetic island prevented by both the large guide field and the electron back pressure is unlikely to independently generate such high-energy electrons either. Based on the observations, our simulations clearly conclude that the generation of energetic electrons in the solar wind is a combined process controlled by both the reconnection electric field and the Fermi-type mechanism, and the trapping effect of the multi-islands configuration maintains the acceleration status that boosts the finally reached energy.

Meanwhile, we also compare our results with the PIC simulations. As seen in Fig. 3.5, the upper panel shows the energy gaining process of the accelerated electrons in our test particle simulation based on MHD simulation. It can be seen that the electrons mainly gain energy near the ends of the magnetic islands, and the kinetic energy in the parallel direction is scattered to the perpendicular direction. These phenomena are the same as those in the PIC simulations (Drake et al. 2006). Certainly, although our simulation results correspond well with the related observations, more self-consistent computations together with detailed observations inside the reconnection diffusion region should be provided.

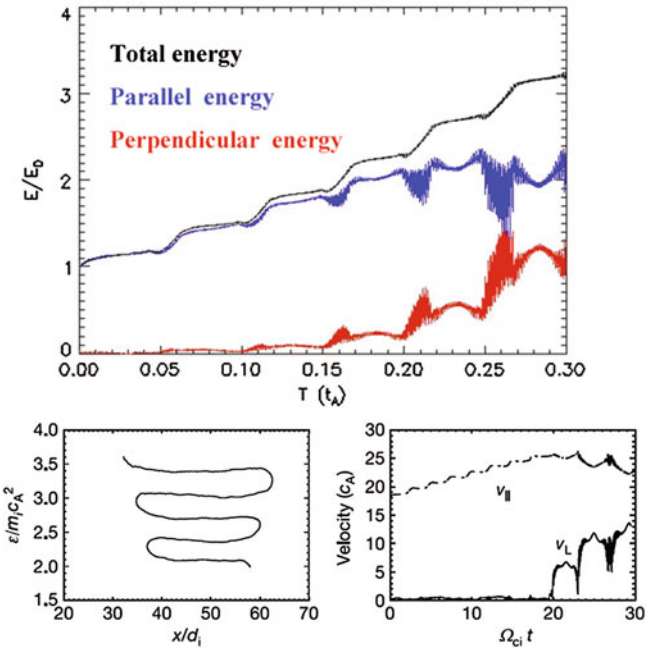

Fig. 3.5 (*upper panel*) electron energy as a function of time in our simulation. (*lower panel*) electron energy as a function of position (*left*) and time (*right*) in PIC simulation. Reprinted with permission from Macmillan Publishers Ltd: (Drake et al. 2006) copyright 2006

In summary, the electric field acceleration and Fermi-type mechanism are two fundamental elements in the electron acceleration in interplanetary magnetic reconnection process, and the trapping effect of the specific magnetic field configuration maintains the acceleration status that increases the totally gained energy.

References

Ambrosiano, J., Matthaeus, W.H., Goldstein, M.L., Plante, D.: Test particle acceleration in turbulent reconnecting magnetic fields. J. Geophys. Res. **93**(A12), 14383–14400 (1988). doi:10.1029/JA093iA12p14383

Birn, J., Drake, J.F., Shay, M.A., Rogers, B.N., Denton, R.E., Hesse, M., Kuznetsova, M., Ma, Z. W., Bhattacharjee, A., Otto, A., Pritchett, P.L.: Geospace environmental modeling (gem) magnetic reconnection challenge. J. Geophys. Res. **106**(A3), 3715–3719 (2001). doi:10.1029/1999ja900449

Birn, J., Priest, E.R.: Reconnection of magnetic fields: magnetohydrodynamics and collisionless theory and observations. Cambridge University Press, Cambridge (2007)

Birn, J., Thomsen, M.F., Borovsky, J.E., Reeves, G.D., Hesse, M.: Particle acceleration in the dynamic magnetotail. Phys. Plasmas **7**(5), 2149–2156 (2000). doi:10.1063/1.874035

Birn, J., Thomsen, M.F., Hesse, M.: Electron acceleration in the dynamic magnetotail: test particle orbits in three-dimensional magnetohydrodynamic simulation fields. Phys. Plasmas **11**(5), 1825–1833 (2004). doi:10.1063/1.1704641

Blackman, E.G., Field, G.B.: Nonthermal acceleration from reconnection shocks. Phys. Rev. Lett. **73**(23), 3097–3100 (1994). doi:10.1103/PhysRevLett.73.3097

Chen, L.J., Bhattacharjee, A., Puhl-Quinn, P.A., Yang, H., Bessho, N., Imada, S., Muehlbachler, S., Daly, P.W., Lefebvre, B., Khotyaintsev, Y., Vaivads, A., Fazakerley, A., Georgescu, E.: Observation of energetic electrons within magnetic islands. Nat. Phys. **4**(1), 19–23 (2008). doi:10.1038/Nphys777

Dmitruk, P., Matthaeus, W.H., Seenu, N.: Test particle energization by current sheets and nonuniform fields in magnetohydrodynamic turbulence. Astrophys. J. **617**(1), 667 (2004). doi:10.1086/425301

Drake, J.F., Swisdak, M., Cattell, C., Shay, M.A., Rogers, B.N., Zeiler, A.: Formation of electron holes and particle energization during magnetic reconnection. Science **299**(5608), 873–877 (2003). doi:10.1126/science.1080333

Drake, J.F., Swisdak, M., Che, H., Shay, M.A.: Electron acceleration from contracting magnetic islands during reconnection. Nature **443**(7111), 553–556 (2006). doi:10.1038/nature05116

Goldstein, M.L., Matthaeus, W.H., Ambrosiano, J.J.: Acceleration of charged particles in magnetic reconnection: Solar flares, the magnetosphere, and solar wind. Geophys. Res. Lett. **13**(3), 205–208 (1986). doi:10.1029/GL013i003p00205

Gosling, J.T.: Magnetic reconnection in the solar wind. Space Sci. Rev. 1–14 (2011). doi:10.1007/s11214-011-9747-2

Gosling, J.T., Eriksson, S., Blush, L.M., Phan, T.D., Luhmann, J.G., McComas, D.J., Skoug, R. M., Acuna, M.H., Russell, C.T., Simunac, K.D.: Five spacecraft observations of oppositely directed exhaust jets from a magnetic reconnection X-line extending $> 4.26 \times 10^6$ km in the solar wind at 1 AU. Geophys. Res. Lett. **34**(20), L20108 (2007). doi:10.1029/2007gl031492

Gosling, J.T., Skoug, R.M., Haggerty, D.K., McComas, D.J.: Absence of energetic particle effects associated with magnetic reconnection exhausts in the solar wind. Geophys. Res. Lett. **32**(14), L14113 (2005). doi:10.1029/2005gl023357

Hoshino, M.: Electron surfing acceleration in magnetic reconnection. J. Geophys. Res. **110**(A10), A10215 (2005). doi:10.1029/2005ja011229

Hoshino, M.: Stochastic particle acceleration in multiple magnetic islands during reconnection. Phys. Rev. Lett. **108**(13), 135003 (2012). doi:10.1103/PhysRevLett.108.135003

Hoshino, M., Mukai, T., Terasawa, T., Shinohara, I.: Suprathermal electron acceleration in magnetic reconnection. J. Geophys. Res. **106**(A11), 25979–25997 (2001). doi:10.1029/2001ja900052

Imada, S., Nakamura, R., Daly, P.W., Hoshino, M., Baumjohann, W., Mühlbachler, S., Balogh, A., Rème, H.: Energetic electron acceleration in the downstream reconnection outflow region. J. Geophys. Res. **112**(A3), A03202 (2007). doi:10.1029/2006ja011847

Lavraud, B., Gosling, J., Rouillard, A., Fedorov, A., Opitz, A., Sauvaud, J.A., Foullon, C., Dandouras, I., Génot, V., Jacquey, C., Louarn, P., Mazelle, C., Penou, E., Phan, T., Larson, D., Luhmann, J., Schroeder, P., Skoug, R., Steinberg, J., Russell, C.: Observation of a complex solar wind reconnection exhaust from spacecraft separated by over 1800 RE. Sol. Phys. **256**(1), 379–392 (2009). doi:10.1007/s11207-009-9341-x

Liu, C.X., Jin, S.P., Wei, F.S., Lu, Q.M., Yang, H.A.: Plasmoid-like structures in multiple X line Hall MHD reconnection. J. Geophys. Res. **114**(A10), A10208 (2009). doi:10.1029/2009ja014257

Matthaeus, W.H., Ambrosiano, J.J., Goldstein, M.L.: Particle acceleration by turbulent magnetohydrodynamic reconnection. Phys. Rev. Lett. **53**(15), 1449–1452 (1984). doi:10.1103/PhysRevLett.53.1449

Oka, M., Fujimoto, M., Shinohara, I., Phan, T.D.: "Island surfing" mechanism of electron acceleration during magnetic reconnection. J. Geophys. Res. **115**(A8), A08223 (2010a). doi:10.1029/2010ja015392

Oka, M., Phan, T.-D., Krucker, S., Fujimoto, M., Shinohara, I.: Electron acceleration by multi-island coalescence. Astrophys. J. **714**(1), 915 (2010b). doi:10.1088/0004-637X/714/1/915

Phan, T.D., Gosling, J.T., Davis, M.S., Skoug, R.M., Oieroset, M., Lin, R.P., Lepping, R.P., McComas, D.J., Smith, C.W., Reme, H., Balogh, A.: A magnetic reconnection X-line extending more than 390 Earth radii in the solar wind. Nature **439**(7073), 175–178 (2006). doi:10.1038/nature04393

Pritchett, P.L.: Relativistic electron production during driven magnetic reconnection. Geophys. Res. Lett. **33**(13), L13104 (2006a). doi:10.1029/2005gl025267

Pritchett, P.L.: Relativistic electron production during guide field magnetic reconnection. J. Geophys. Res. **111**(A10), A10212 (2006b). doi:10.1029/2006ja011793

Pritchett, P.L.: Energetic electron acceleration during multi-island coalescence. Phys. Plasmas **15**(10), 102105–102109 (2008). doi:10.1063/1.2996321

Sonnerup, B.U.Ö.: Adiabatic particle orbits in a magnetic null sheet. J. Geophys. Res. **76**(34), 8211–8222 (1971). doi:10.1029/JA076i034p08211

Speiser, T.W.: Particle trajectories in model current sheets 1. Analytical Solutions. J. Geophys. Res. **70**(17), 4219–4226 (1965). doi:10.1029/JZ070i017p04219

Wang, Y., Wei, F.S., Feng, X.S., Zhang, S.H., Zuo, P.B., Sun, T.R.: Energetic electrons associated with magnetic reconnection in the magnetic cloud boundary layer. Phys. Rev. Lett. **105**(19), 195007 (2010). doi:10.1103/PhysRevLett.105.195007

Wei, F.S., Liu, R., Feng, X., Zhong, D., Yang, F.: Magnetic structures inside boundary layers of magnetic clouds. Geophys. Res. Lett. **30**(24), 2283 (2003). doi:10.1029/2003gl018116

Zhang, S.-H., Feng, X.-S., Wang, Y., Yang, L.-P.: Magnetic reconnection under solar coronal conditions with the 2.5D AMR resistive MHD model. Chin. Phys. Lett. **28**(8) (2011). doi:10.1088/0256-307x/28/8/089601

Chapter 4
Proton and Electron Flux Variations in the Magnetic Cloud Boundary Layers

4.1 Introduction

Magnetic cloud boundary layer is a distinct region formed by the interaction of the magnetic cloud (MC) and the solar wind. To our knowledge, the concept of BL is proposed from the discussions about the criteria for identifying the MC boundary (Wei et al. 2003b). In the past few years, research on BL has mainly focused on its macroscopical characteristics such as magnetic field structures, plasma environment and the associated waves (Wei et al. 2003a, b, c, 2005, 2006). To get a comprehensive and insightful understanding of the BL, studies on the microcosmic characteristics of the BL are needed (Wang et al. 2012).

Investigating the plasma velocity distribution function (VDF) is an effective way to diagnose the plasma structure in the solar wind, since the density and temperature are macroscopic manifestations of the plasma VDF (Paschmann and Daly 1998). In addition, magnetic field lines are 'frozen' into the plasma in the solar wind. So the behaviors of magnetic field should also be related to the local plasma VDF. Therefore, it should be interesting and significant to analyze the proton and electron flux variations in the BL.

4.2 The Velocity Distribution Function

4.2.1 Definition of the Velocity Distribution Function

Plasma VDF describes the distribution of position and velocity in phase space. The Maxwell distribution is the simplest case which implies that particles are assumed to have reached thermodynamic equilibrium. The VDF can be written as

© Springer-Verlag Berlin Heidelberg 2016

Y. Wang, *Magnetic Cloud Boundary Layers and Magnetic Reconnection*,
Springer Theses, DOI 10.1007/978-3-662-48310-7_4

$$f(v) = n(\frac{m}{2\pi k_B T})^{\frac{3}{2}} \exp(-\frac{mv^2}{2k_B T})$$

where k_B is the Boltzmann constant. Figure 4.1 illustrates six typical VDFs in $(v_\perp, v_\parallel)$ space.

4.2.2 The Moments of the Velocity Distribution Function

Plasma density, bulk velocity, pressure, and temperature can be calculated from the VDF. The zeroth order moment of the VDF is the density

$$N = \int f(v) \mathrm{d}^3 v$$

The plasma bulk velocity can be defined as

$$V = \frac{\int f(v) v \mathrm{d}^3 v}{\int f(v) \mathrm{d}^3 v}$$

Then the pressure can be deduced from V

$$P = m \int f(v)(v - V)(v - V) \mathrm{d}^3 v$$

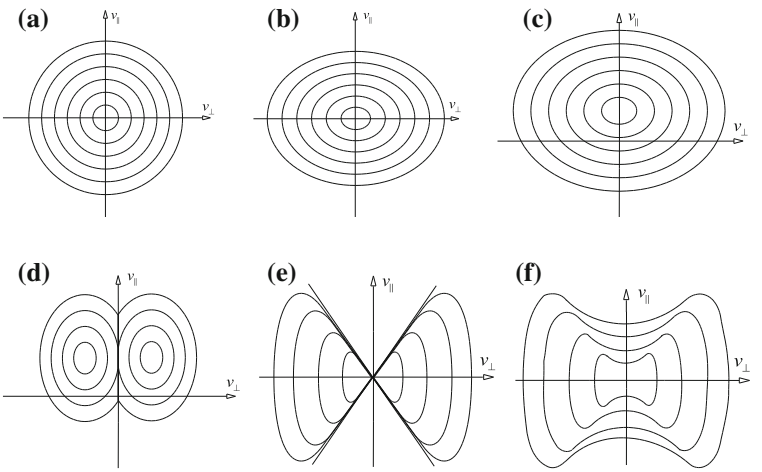

Fig. 4.1 Contours of typical VDF. Here, **a–f** are Maxwell distribution, Bi-Maxwell distribution, beam distribution, ring-beam distribution, loss-cone distribution, and partially-filled loss-cone distribution, respectively

Correspondingly, the moment temperature can be calculated as

$$T = P/(Nk)$$

We can see that the macroscopical characteristics are closely related to the VDF.

4.2.3 *Electron Velocity Distribution Function in Solar Wind*

In solar wind, electron VDF usually has two components (Feldman et al. 1983; Larson et al. 1997; Phillips and Gosling 1990; Pierrard et al. 2001; Pilipp et al. 1987), a collisional hot core (core electrons, $T < \sim 70$ eV) and a nearly collisionless suprathermal tail (suprathermal electrons, $T > \sim 70$ eV). In addition, the suprathermal electrons can be further classified into two categories: a nearly isotropic component (halo electrons) and a relatively strong beam component (strahl electrons). Figure 4.2 shows the different electron components.

Generally, the VDF of the observed core electrons in the solar wind can be fitted by the Maxwell distribution, and the fitted temperature is called core temperature. The core temperature is usually cooler than the moment temperature.

The strahl electrons are widely used to diagnose the magnetic field configuration in the solar wind (Gosling et al. 2005; Larson et al. 1997; Phillips and Gosling 1990; Pierrard et al. 2001; Pilipp et al. 1987). For example, the bidirectional

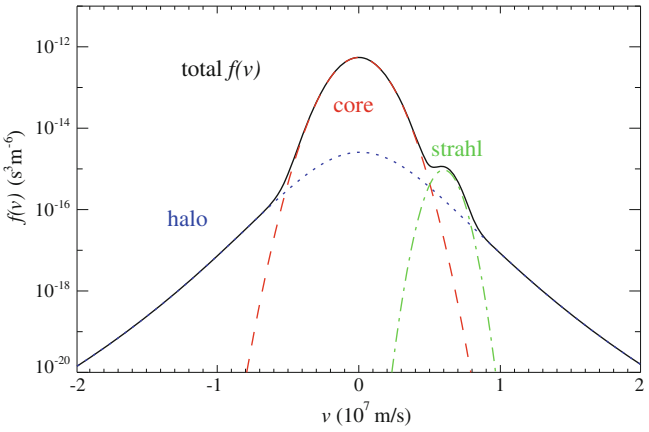

Fig. 4.2 Typical electron VDF in the solar wind. Different electron components are marked by different colors

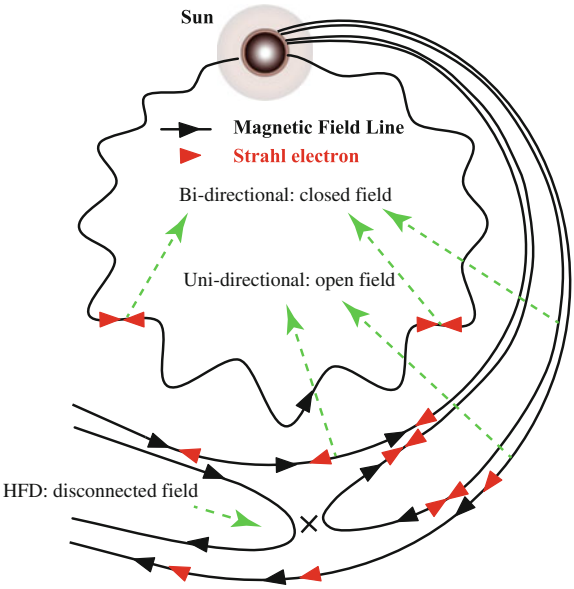

Fig. 4.3 Strahl electrons and the possible topology of the magnetic field lines

suprathermal electrons, unidirectional suprathermal electron beam, and the heat flux dropout (HFD)[1] are possible evidences revealing whether the magnetic field lines are connected directly to the sun (see Fig. 4.3).

4.3 Data Set Description

4.3.1 Instruments and Data

The data referred in this chapter are obtained from the WIND 3-D Plasma and energetic particle experiment (3DP) (Lin et al. 1995). We will analyze the flux data provided by the electron electrostatic analyzers (EESA), ion electrostatic analyzers (PESA), and semiconductor telescopes (SST). To the electrons, the VDF data provided by WIND is gyrotropic, while to the protons, we only get the omnidirectional data. To facilitate the statistical analyses, we select four directions and rebuild the energy bands (listed in Table 4.1). In addition, data obtained from EESA-H and PLSP are abandoned since there are too many invalid data gaps. Finally, 18 eV–500 keV electrons in parallel, perpendicular, and antiparallel directions and 4 keV–4 MeV protons in omnidirection will be analyzed.

[1] *Note* The electron heat flux is defined as $H = \frac{m}{2}\int f(v)|v - V|^2(v - V)\mathrm{d}^3v$. Only the asymmetry components with respect to V in $f(v)$ will contribute to the integration, and the strahl electrons are just the asymmetry ones in VDF. So the flux variations of the strahl electrons could be reflected by the heat flux variation.

Table 4.1 The selected energy bands on WIND/3DP and the corresponding instruments

Category (direction)	Electron (parallel, perpendicular, antiparallel)		Proton (omni)	
Instrument (source)	EESA-L (ELPD) (eV)	SST-F (SFPD) (KeV)	PESA-H (PHSP) (KeV)	SST-MO (SOSP) (KeV)
Energy bands	18			
	27	27	4	74
	42	40	6	128
	65	66	9	197
	103	108	11	333
	165	183	15	552
	265	307	21	1018
	427	512	28	2074
	689			4440

4.3.2 *Event Selection*

We only analyze the particle flux variations in the front BL[2] since the characteristics of the tail BL are a bit different. We select 41 typical BL events (listed in Table 4.2) throughout an entire solar cycle. All the BL events are determined by the descriptions given by (Wei et al. 2003b).

Statistical analyses require proper quantities that can characterize the main features of the samples. Since this work aims at researching the changes of fluxes in the BL with respect to the ambient solar wind, we prefer to quantify the flux variations in the form of $\Delta F = (F_2 - F_1)/F_1$ at all the energy bands, where F_1 represents the average flux in the BL, and F_2 denotes the nearby upstream solar wind with 30 min duration. The change of magnetic field and plasma parameters are also described by such a rule.

4.4 Statistical Results

As shown in Table 4.2, the average duration time of the BL is about 1 h. Magnetic field usually decreases inside the BL ($\Delta Bt \sim -16.4$ %). The plasma is also compressed and heated (Np, Tp, Te $\sim$ 42.9, $\sim$ 16.6, and magnetic field conditions near $\sim$ 5.3 %, respectively). These features consist well with previous reports and they are manifestations of the possible magnetic reconnection processes (Wei et al. 2003a, b, c).

[2]*Note* All the 'BL' referred in Chaps. 4 and 5 indicate the front BL by default if they are not specified.

Table 4.2 41 typical BL events observed by WIND

No.[a]	DATE[b]	Start[c]	Dur[d]	ΔBt[e]	|ΔVp|[f]	ΔNp[g]	ΔTe[h]	ΔTp[i]
1	19950208	0252	31	−8.09	6.58	17.31	−4.57	−4.28
2	19950403	0629	75	−12.91	1.70	40.91	0.22	19.85
3	19950822	2036	61	−3.76	1.53	10.24	−2.40	5.61
4	19951018	1820	41	−22.24	2.38	4.15	−0.62	1.94
5	19960527	1210	152	−21.89	2.09	93.15	−3.45	7.16
6	19960701	1546	100	−17.55	9.92	4.22	−1.03	−0.47
7	19970411	0524	30	8.21	0.36	−8.47	−2.69	21.94
8	19970421	1152	13	−30.56	2.36	7.40	−2.37	12.08
9	19970515	0732	139	−16.73	32.64	−22.53	18.07	154.98
10	19970715	0844	21	−36.69	3.50	88.51	0.16	11.94
11	19970803	1005	226	−4.81	12.72	133.46	−16.20	−1.53
12	19970918	0255	57	−18.28	7.70	40.77	2.92	17.14
13	19971107	1438	59	−1.20	0.45	21.52	−7.61	−0.97
14	19971122	1448	22	−15.12	23.70	49.51	9.73	53.52
15	19980502	1233	21	−4.18	5.43	30.12	1.24	3.71
16	19980624	1611	31	−18.36	7.02	40.40	−3.93	−9.90
17	19980820	0450	263	−34.37	35.43	104.60	−6.23	21.38
18	19981108	2250	79	−11.65	5.32	39.97	17.13	23.54
19	19990218	1149	33	−23.58	23.58	41.22	26.70	−2.38
20	19990809	0756	142	−7.00	3.47	30.88	18.78	−6.21
21	20000221	0155	193	−39.13	4.08	55.08	17.96	−27.99
22	20001003	1634	44	−8.62	19.14	5.86	17.81	55.14
23	20010421	2347	25	−13.83	1.40	30.07	10.91	11.76
24	20010710	1638	92	−5.55	4.90	−0.30	2.92	15.44
25	20020319	2127	131	−18.96	5.86	2.80	4.54	42.80
26	20020324	0305	14	−21.83	4.72	123.21	23.79	32.09
27	20020418	0419	20	−19.89	17.98	17.93	4.49	61.71
28	20020519	0246	34	−33.36	14.79	43.60	12.33	5.87
29	20020801	1119	26	−22.67	9.31	48.73	25.64	23.08
30	20020802	0604	71	−6.07	1.46	21.70	1.64	18.36
31	20020903	0250	71	4.21	9.44	33.34	18.89	−7.48
32	20040404	0205	18	−18.46	33.65	191.12	1.19	62.40
33	20040722	1258	56	−28.26	27.65	36.16	15.41	−14.50
34	20040724	1129	27	−9.27	12.78	−10.59	−5.54	10.99
35	20040829	1830	28	−18.18	33.78	0.17	−1.02	0.54
36	20041109	1937	53	−41.59	5.98	68.43	20.51	13.83
37	20050520	0604	42	−17.01	2.46	29.97	−7.81	14.32
38	20050612	1441	21	−44.36	81.13	54.60	−2.16	10.77
39	20051231	1233	76	−37.93	6.83	187.31	16.98	7.20
40	20060205	1759	63	3.36	0.57	5.47	−10.34	−13.15

(continued)

Table 4.2 (continued)

No.[a]	DATE[b]	Start[c]	Dur[d]	ΔBt[e]	|ΔVp|[f]	ΔNp[g]	ΔTe[h]	ΔTp[i]
41	20060413	2023	41	−3.65	8.08	46.47	5.87	29.96
AVERAGE			67	−16.39	12.05	42.89	5.31	16.64

[a]Event number
[b]The date of event, formatted as Year/Month/Day
[c]The beginning time of the event, formatted as Hour/Minute (UT)
[d]Event duration (minute)
[e]The change of total magnetic field (%)
[f]The absolute difference of proton velocity (km/s)
[g]The change of proton density (%) (Here, the proton density and electron density are assumed to be equal, so are in Chap. 5. The electron density in the solar wind is discussed in Sect. 4.6.)
[h]The change of electron temperature (%)
[i]The change of proton temperature (%)

Electron flux variations in parallel, perpendicular, and antiparallel directions and proton flux in omnidirection at different energy bands are shown in Fig. 4.4. It is found that the flux variations behave differently in different directions and at different energy bands. Such features imply strong energy dependency and direction selectivity. Specifically, (1) the core electrons show similar flux variations in three different directions and the increment amplitude decreases with energy monotonously from ∼30 % (at 18 eV) to ∼10 % (at 70 eV); (2) the increments of suprathermal electron (100–700 eV) in the parallel and antiparallel directions are very small (<4 %), but it is noted that their standard errors are obviously large; (3) the energetic electron (>100 keV) also has slight increments in the perpendicular

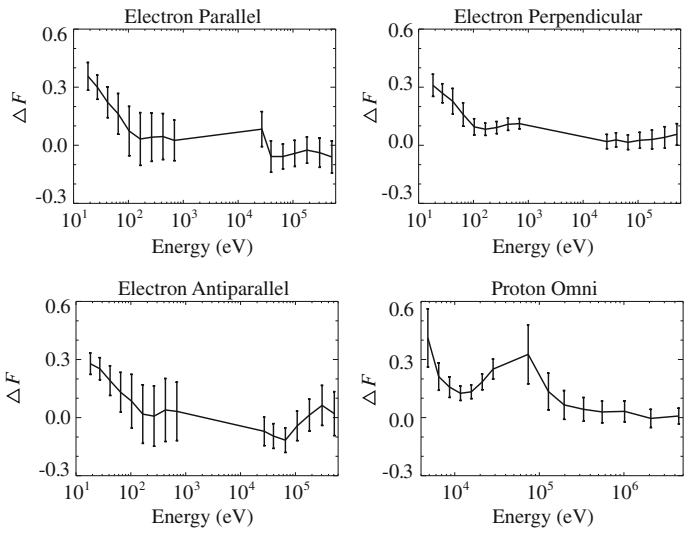

Fig. 4.4 Normalized particle flux variations with error bars at each energy band

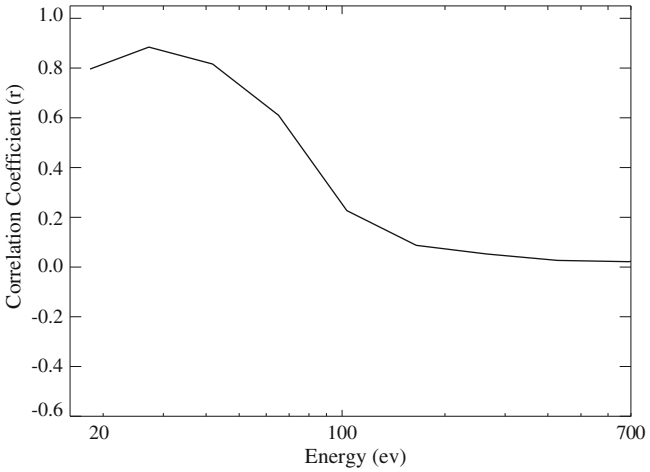

Fig. 4.5 Correlation coefficients of electron flux variations in the parallel and antiparallel directions as a function of energy

direction; (4) the increments of the proton omni flux fall at higher energy bands, but they have a prominence around 70 keV.

For further analyses of particle flux variations, we calculate the correlation coefficients of electron flux variations in the parallel and antiparallel directions. As shown in Fig. 4.5, the core electron has (strong) positive correlations ($r > 0.8$) in the parallel and antiparallel directions. The correlation coefficients change sharply around 70 eV, and the suprathermal electron has very low or negative correlations ($r \sim 0$).

4.5 Explanations for the Flux Variations at Different Energy Bands

4.5.1 The Core Electrons

The core electron flux variations in the BL should be closely related to the plasma density, since zeroth order moment of the VDF is equal to the density. If the VDF of the plasma is assumed to have a Maxwell distribution, the density will behave essentially the same as the flux. In other words, the lower the flux energy is, the more similar behaviors the density and flux will have (see Fig. 4.6).

This phenomenon is usually found in solar wind, as seen in Fig. 4.7; the isotropic increments of electron flux at 15–41 eV vary consistently with the density changes in the BL. It is noteworthy that, the average density increment of 41 BL events is $\sim$42.9 %, which is also roughly consistent with the final increment of the electron flux at 18 eV ($\sim$30 %). Actually, as stated above, electron fluxes at lower

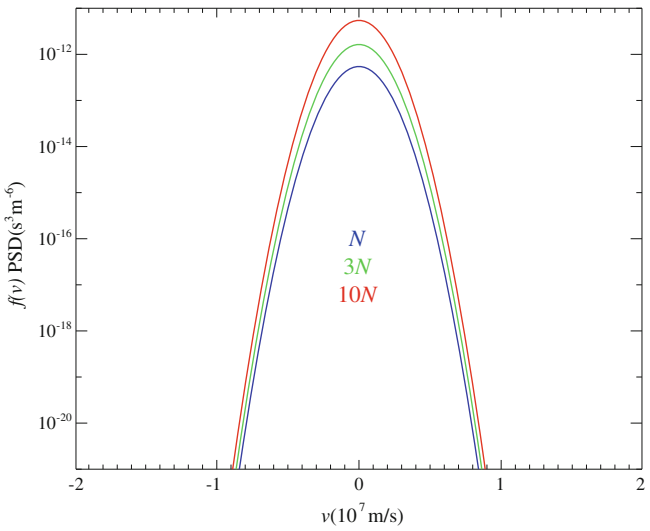

Fig. 4.6 VDF with different density (N, 3 N, 10 N) under the same temperature condition

energy bands will behave even more similar to the density, but we do not use the electron flux data under 18 eV (the reason will be discussed in Sect. 4.6).

4.5.2 The Suprathermal Electrons

As described above, the bidirectional suprathermal electrons, unidirectional suprathermal electrons, and the absence of Strahl electrons are useful information to infer the configurations of closed, open, and disconnected magnetic field lines from the Sun. It is quite possible that the flux variations of the suprathermal electrons in Fig. 4.4 as well as the near zero correlation coefficients in Fig. 4.5 also result from the topological change of the magnetic field lines. In statistics, the enhancements of the strahl electrons, mainly concentrating in the parallel direction will counteract those enhancements mainly concentrating in the antiparallel direction. Hence, the final average enhancements should be near zero and the standard error will be large. Referring to Fig. 4.3, if the spacecraft detects unidirectional suprathermal electrons in the solar wind first, thereafter, it observes bidirectional suprathermal electrons or HFD in the BL (see Fig. 4.8). Then the calculated correlation coefficients of suprathermal electron flux variations in the parallel and antiparallel directions will be very low. This feature is just reflected in Fig. 4.5. Therefore, flux variations of the suprathermal electron can indicate the topological change of the magnetic field lines such as the possible magnetic reconnection processes as discussed in previous work (Wei et al. 2006, 2003a, b, c).

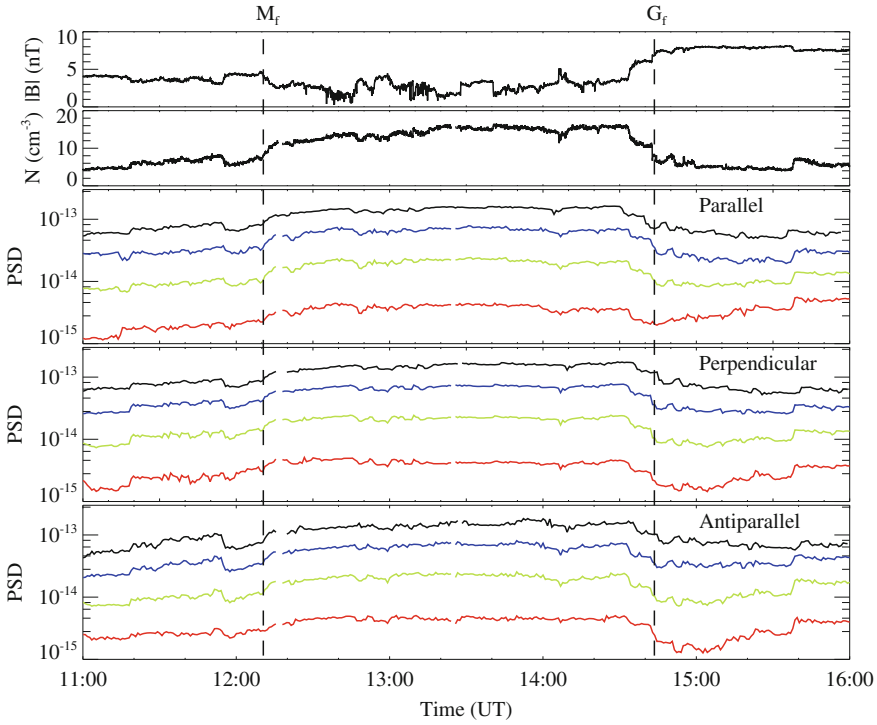

Fig. 4.7 Plasma and magnetic field conditions near the BL on May 27, 1996 (marked by M_f and G_f, *dashed lines*). From *top* to *bottom* the magnitude of magnetic field, electron density, and electron flux in parallel, perpendicular, and antiparallel directions. The color lines represent different energy bands at 15 eV (*black*), 21 eV (*blue*), 29 eV (*yellow*), and 41 eV (*red*), respectively

4.5.3 Energetic Electrons

The flux enhancement of the energetic electrons and its standard error are both small. These results imply that there is indeed no obvious flux enhancement of the energetic electrons inside the BL. However, it may also be possible that the energetic electrons have pulsing flux enhancement inside some BL events (Wang et al. 2010), but the averaged flux variations are small due to the long duration of the BL.

4.5.4 Protons

Since the directional data of the proton flux is unavailable to us and the data provided by PESA-L and PESA-H (lower energy bands) is unreliable either, it is difficult to

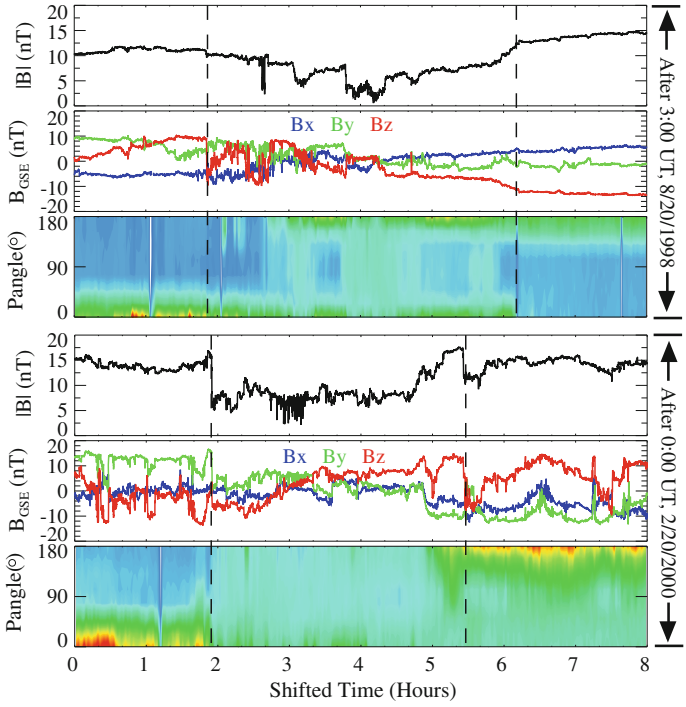

Fig. 4.8 Bidirectional (*upper panel*) suprathermal electrons and HFD (*lower panel*) at ~260 eV in the BL. Different colors in the contours denote different flux intensity (*red* strong, *blue* weak)

have a comprehensive analyses on the proton flux. However, it is noted that there is a peak value around 70 keV in Fig. 4.4. This phenomenon is also observed in the interplanetary magnetic reconnection exhaust as reported in Chap. 2.

4.6 Discussion and Summary

Since the flux of electrons in low-energy band (~<10–20 eV) is usually affected by the photoelectron of the spacecraft, the data provided by WIND/3DP should be carefully calibrated before using (Lin et al. 1995; Paschmann and Daly 1998; Pedersen et al. 2008). A possible solution is to fit the VDF of the electrons by Gaussian distribution. However, this method is a bit complex and the validity is not fully guaranteed in statistical work. So we do not consider the electron data below 18 eV. In addition, we abandon the data provided by EESA-H because of the frequently occurred invalid data. Overall, these processes do not affect the major results of our work.

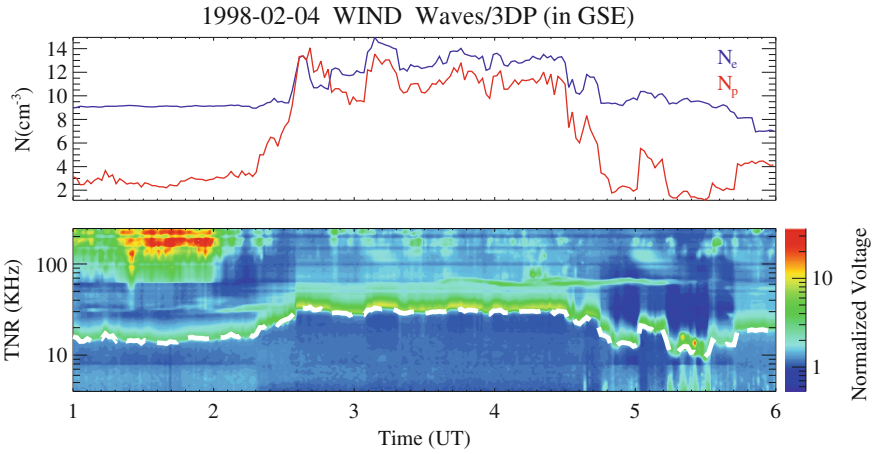

Fig. 4.9 (*upper panel*) Density of electrons and protons directly obtained from the spacecraft (*lower panel*) wave spectrum. The *white dashed line* is the electron density deduced from the 'plasma line'

Although plasma is electrically neutral, the electron density directly obtained from the spacecraft is not exactly the same as the proton density, and it also needs calibrations (Paschmann and Daly 1998). The wave spectrum can be used to calibrate the electron density. As seen in Fig. 4.9, in the solar wind, the Langmuir waves will display a bright 'plasma line' in the spectrum. So we can deduce the electron density from the plasma frequency

$$f_{pe} = \frac{1}{2\pi}\sqrt{\frac{ne^2}{m\varepsilon_0}}$$

In the statistical work, it is found that the electron density deduced from the 'plasma line' fits well with the proton density in many cases. So, the proton density and electron density are assumed to be equal in Chaps. 4 and 5.

Actually, the averaged flux variation used in data processing will smooth the results. We also adopt another sample method, such as applying the maximum flux in the same time range to the events. Although we get more unsmooth results, the main features also resemble the results presented here.

To sum up, we carry out a statistical study to analyze the proton and electron flux variations inside the 41 BL events on reliable energy bands throughout an entire solar cycle (1995–2006). It is found that the core electron flux increases quasi-isotropically and the increments decrease monotonously with energy from $\sim$30 % (at 18 eV) to $\sim$10 % (at 70 eV); the suprathermal electron flux usually increases in either parallel or antiparallel direction; the correlation coefficients of electron flux variations in parallel and antiparallel directions change sharply from $\sim$0.8 below 70 eV to $\sim$0 above 70 eV; the energetic electron has slight increments

in the perpendicular direction; the increments of the proton omni flux have a prominence around 70 keV. These features indicate that magnetic field lines may break up or reverse inside the BL. Considering the work done before, it is inferred that magnetic reconnection processes may occur frequently in the BL.

References

Feldman, W.C., Anderson, R.C., Bame, S.J., Gosling, J.T., Zwickl, R.D., Smith, E.J.: Electron velocity distributions near interplantary shocks. J. Geophys. Res. **88**(A12), 9949–9958 (1983). doi:10.1029/JA088iA12p09949

Gosling, J.T., Skoug, R.M., McComas, D.J., Smith, C.W.: Magnetic disconnection from the sun: observations of a reconnection exhaust in the solar wind at the heliospheric current sheet. Geophys. Res. Lett. **32**(5), L05105 (2005). doi:10.1029/2005gl022406

Larson, D.E., Lin, R.P., McTiernan, J.M., McFadden, J.P., Ergun, R.E., McCarthy, M., Rème, H., Sanderson, T.R., Kaiser, M., Lepping, R.P., Mazur, J.: Tracing the topology of the October 18–20, 1995, magnetic cloud with $\sim 0.1–10^2$ keV electrons. Geophys. Res. Lett. **24**(15), 1911–1914 (1997). doi:10.1029/97gl01878

Lin, R.P., Anderson, K.A., Ashford, S., Carlson, C., Curtis, D., Ergun, R., Larson, D., McFadden, J., McCarthy, M., Parks, G.K., Rème, H., Bosqued, J.M., Coutelier, J., Cotin, F., D'Uston, C., Wenzel, K.P., Sanderson, T.R., Henrion, J., Ronnet, J.C., Paschmann, G.: A three-dimensional plasma and energetic particle investigation for the wind spacecraft. Space Sci. Rev. **71**(1), 125–153 (1995). doi:10.1007/bf00751328

Paschmann, G., Daly, P.W.: Analysis Methods for Multi-Spacecraft Data. ESA Publications Division, Bern (1998)

Pedersen, A., Lybekk, B., André, M., Eriksson, A., Masson, A., Mozer, F.S., Lindqvist, P.A., Décréau, P.M.E., Dandouras, I., Sauvaud, J.A., Fazakerley, A., Taylor, M., Paschmann, G., Svenes, K.R., Torkar, K., Whipple, E.: Electron density estimations derived from spacecraft potential measurements on Cluster in tenuous plasma regions. J. Geophys. Res. **113**(A7), A07S33 (2008). doi:10.1029/2007ja012636

Phillips, J.L., Gosling, J.T.: Radial evolution of solar wind thermal electron distributions due to expansion and collisions. J. Geophys. Res. **95**(A4), 4217–4228 (1990). doi:10.1029/JA095iA04p04217

Pierrard, V., Maksimovic, M., Lemaire, J.: Core, halo and strahl electrons in the solar wind. Astrophys. Space Sci. **277**(1), 195–200 (2001). doi:10.1023/a:1012218600882

Pilipp, W.G., Miggenrieder, H., Montgomery, M.D., Mühlhäuser, K.H., Rosenbauer, H., Schwenn, R.: Characteristics of electron velocity distribution functions in the solar wind derived from the helios plasma experiment. J. Geophys. Res. **92**(A2), 1075–1092 (1987). doi:10.1029/JA092iA02p01075

Wang, Y., Wei, F.S., Feng, X.S., Zhang, S.H., Zuo, P.B., Sun, T.R.: Energetic electrons associated with magnetic reconnection in the magnetic cloud boundary layer. Phys. Rev. Lett. **105**(19), 195007 (2010). doi:10.1103/PhysRevLett.105.195007

Wang, Y., Wei, F.S., Feng, X.S., Zuo, P.B., Guo, J.P., Xu, X.J., Li, Z.: Variations of solar electron and proton flux in magnetic cloud boundary layers and comparisons with those across the shocks and in the reconnection exhausts. Astrophys. J. **749**(1), 82 (2012). doi:10.1088/0004-637X/749/1/82

Wei, F.S., Feng, X., Yang, F., Zhong, D.: A new non-pressure-balanced structure in interplanetary space: boundary layers of magnetic clouds. J. Geophys. Res. **111**(A3), A03102 (2006). doi:10.1029/2005ja011272

Wei, F.S., Hu, Q., Feng, X., Fan, Q.: Magnetic reconnection phenomena in interplanetary space. Space Sci. Rev. **107**(1), 107–110 (2003a). doi:10.1023/a:1025563420343

Wei, F.S., Liu, R., Fan, Q., Feng, X.: Identification of the magnetic cloud boundary layers. J. Geophys. Res. **108**(A6), 1263 (2003b). doi:10.1029/2002ja009511

Wei, F.S., Liu, R., Feng, X., Zhong, D., Yang, F.: Magnetic structures inside boundary layers of magnetic clouds. Geophys. Res. Lett. **30**(24), 2283 (2003c). doi:10.1029/2003gl018116

Wei, F.S., Zhong, D., Feng, X., Yang, F.: WIND observations of plasma waves inside the magnetic cloud boundary layers. Chin. Sci. Bull. **50**(17), 1906–1911 (2005). doi:10.1360/982004-577

Chapter 5
The Criterion of Magnetic Reconnection in the Solar Wind

5.1 Introduction

Ever since the "direct evidence" of magnetic reconnection in the solar wind has been proposed by Gosling et al. (2005a), many reconnection exhausts are reported (Gosling et al. 2005a, b; Davis et al. 2006; Phan et al. 2006; Gosling et al. 2007a, b; Huttunen et al. 2007; Lavraud et al. 2009; Tian et al. 2010; Wang et al. 2010; Gosling 2011; Xu et al. 2011). However, it is very difficult for the spacecraft to detect direct reconnection evidence such as the hall signatures as those in the magnetotail (Birn and Priest 2007) since the reconnection diffusion region is quite small in the solar wind. So the key evidence for identifying the magnetic reconnection in the solar wind becomes to find the Alfvénic reconnection jets calculated by Walen relation in the reconnection exhaust as pointed in the review article (Gosling 2011).

Early observations (McComas et al. 1994) show that the fast ICME propagating in the solar wind will compress the ambient solar wind, and then magnetic reconnection may take place in front of the ICME. The compressing effect of the ICME behaving as the driving flows in magnetic reconnection may help promote its initiation, and such scenario has been demonstrated by observations and numerical simulations (Dasso et al. 2006; Wang et al. 2010; Wei et al. 2003a, b). However, recently, statistical work (Gosling 2011; Gosling et al. 2007b) indicates that the solar wind magnetic reconnection will be suppressed in high beta value plasma, and particularly, it prefers occurring spontaneously inside the ICME where the solar wind generally has low beta value instead of ahead of the ICME.

This problem arouses our interests in discussing the criterion of magnetic reconnection in the solar wind. Actually, the interaction region between the ICME and the solar wind, which is similar to the BL region discussed in the previous chapters, is a dynamic region where the magnetic field and plasma parameters

© Springer-Verlag Berlin Heidelberg 2016

Y. Wang, *Magnetic Cloud Boundary Layers and Magnetic Reconnection*,
Springer Theses, DOI 10.1007/978-3-662-48310-7_5

change complexly. To a single spacecraft, the "direct evidence" referred above may not really reflect the physical processes in such region. Moreover, it should not be ignored that the measured reconnection jets are not well-consistent with the roughly Alfvénic accelerated flows calculated by Walen relation in some reported reconnection events. The discrepancy between the observations and calculations can even exceed 40 % in certain events. These analyses bring about an interesting question: besides the Alfvénic accelerated flows, can other characteristics be selected as the proper criterion of magnetic reconnection in the solar wind?

Magnetic field, plasma density, temperature, and velocity will change during the magnetic reconnection processes. Generally, it is hard to identify a reconnection event by only using the magnetic field signatures (Gosling 2011). Since the plasma density, temperature, and velocity can all be calculated from the particle VDF, it is speculated that variations of particle flux may also be useful signatures for identifying the reconnection event.

In this chapter, we compare the proton and electron mean flux variations in the BL, in the interplanetary reconnection exhaust (RE), and across the MC-driven shock by using the Wind 3DP and MFI data from 1995 to 2006. It is found that the strong energy dependence and direction selectivity of electron flux variations, which are previously thought to have no enough relevance to magnetic reconnection, could be considered as an important signature of solar wind reconnection in the statistical point of view.

5.2 Event Selection

The event selection and data processing are similar to those in Chap. 4. The variations of particle flux are denoted by $\Delta F = (F_2 - F_1)/F_1$ at all the energy bands and directions for each event. To the RE, F_2 is the mean flux inside the RE and F_1 is mean flux of the nearby upstream solar wind with the same duration of the RE. For the shock, F_1 and F_2 are the mean flux of upstream and downstream solar wind, respectively, with 12 min duration and 3 min away from the shock discontinuity.

5.2.1 The Reconnection Exhaust

The interplanetary RE events are chosen from the list provided by Huttunen et al. (2007). Since the time resolution of the EESA and PESA is $\sim$98 s, the RE events with too short duration (<98 s) are excluded. The final 24 events are listed in Table 5.1.

Table 5.1 Selected solar wind reconnection exhausts observed by WIND

No.[a]	DATE[b]	Start[c]	Dur[d]	ΔBt[e]	|ΔVp|[f]	ΔNp[g]	ΔTe[h]	ΔTp[i]
1	19971116	164250	220	−38.96	11.13	157.35	30.76	96.31
2	19980416	005434	198	2.27	17.01	−26.45	2.55	96.76
3	19980821	202036	240	−22.31	9.24	37.94	16.54	82.14
4	19980917	033315	109	−14.52	16.27	28.77	−0.15	29.06
5	19990218	102624	218	−23.31	56.20	213.91	63.95	7.90
6	19990615	143235	108	−13.32	16.82	42.82	13.23	91.98
7	19990626	054600	550	−25.24	7.95	29.85	20.53	2.85
8	19990728	043559	189	−24.44	6.29	39.33	1.72	49.62
9	19990810	183820	356	−43.70	2.26	29.98	15.48	16.78
10	19990919	091004	266	−30.09	20.71	24.34	1.90	5.43
11	20000419	035916	194	−39.35	18.40	15.77	10.10	13.30
12	20010617	163023	157	−19.27	38.24	48.55	16.36	1.74
13	20020202	035725	260	−32.48	49.74	65.86	28.72	54.89
14	20020419	004130	300	−9.55	36.29	−14.35	−3.54	10.59
15	20020628	152632	333	−9.36	14.23	22.16	5.92	−11.21
16	20030302	210955	107	−32.84	11.52	6.96	4.90	27.66
17	20040724	115110	235	7.41	62.34	5.42	0.87	45.34
18	20040826	092250	175	−12.69	11.46	−1.11	−3.96	32.22
19	20040914	212651	121	−20.80	60.91	36.30	12.67	−15.88
20	20040919	064100	670	−4.55	12.89	76.63	9.34	5.24
21	20041008	070545	130	−3.13	13.19	13.88	−1.56	6.86
22	20041011	152342	134	−18.82	16.04	−3.39	4.06	−2.68
23	20041029	024531	119	−38.80	9.63	0.77	0.98	1.80
24	20041206	022056	115	−14.50	0.16	2.70	1.95	2.33
AVERAGE			229	−20.09	21.65	35.58	10.56	27.13

[a]Event number
[b]The date of event, formatted as Year/Month/Day
[c]The beginning time of the event, formatted as Hour/Minute/Second (UT)
[d]Event duration (second)
[e]The change of total magnetic field (%)
[f]The absolute difference of proton velocity (km/s)
[g]The change of proton density (%)
[h]The change of electron temperature (%)
[i]The change of proton temperature (%)

5.2.2 *The MC-Driven Shock*

The MC-driven shock events are selected based on the work of Feng et al. (2010). We use the following criteria to select shock events as "MC-driven" events[1]: (1) the

[1]*Note* We also try to use looser conditions ($55° < \theta < 125°$, $t < 16$ h) and more strict conditions ($75° < \theta < 115°$, $t < 12$ h). The major conclusions will not be affected.

Table 5.2 Selected leading shocks ahead of magnetic cloud observed by WIND

No.[a]	DATE[b]	Start[c]	ΔBt[d]	|ΔVp|[e]	ΔNp[f]	ΔTe[g]	ΔTp[h]
1	19950822	1256	85.45	42.38	197.09	14.06	99.64
2	19970109	0052	208.79	28.07	118.19	2.41	139.35
3	19970515	0115	150.20	74.66	89.82	53.27	103.76
4	19970715	0215	19.50	9.90	63.46	10.77	22.35
5	19971010	1557	64.41	24.90	62.48	4.70	27.70
6	19971122	0912	198.94	98.79	144.61	75.63	168.50
7	19980304	1102	84.05	41.99	70.94	41.41	40.19
8	19981018	1929	128.17	30.16	89.00	19.93	57.42
9	20000811	1849	106.38	113.98	90.60	56.96	154.63
10	20010319	1133	107.18	47.99	67.30	70.81	60.64
11	20010404	1441	59.08	211.11	146.90	123.27	327.35
12	20010421	1529	80.23	27.70	115.75	60.64	60.14
13	20011031	1347	64.20	68.53	210.07	54.84	301.31
14	20011124	0454	86.78	75.84	33.69	29.39	46.66
15	20020518	1946	158.76	160.83	202.78	240.26	259.96
16	20020801	0519	57.15	100.17	129.64	34.11	296.22
17	20040724	0531	140.13	68.46	168.05	192.04	267.61
18	20041107	1759	123.46	160.31	142.38	90.91	89.20
19	20050515	0210	484.94	298.62	358.26	469.96	803.67
20	20050612	0648	379.41	37.37	30.07	59.08	48.23
21	20050614	1756	253.53	82.10	78.87	107.21	213.60
22	20060413	1121	113.57	35.12	57.57	45.34	79.13
23	20071119	1722	82.14	34.85	142.13	49.76	42.87
AVERAGE			140.72	81.47	122.16	82.90	161.31

[a]Event number
[b]The date of event, formatted as Year/Month/Day
[c]The beginning time of the event, formatted as Hour/Minute (UT)
[d]The change of total magnetic field (%)
[e]The absolute difference of proton velocity (km/s)
[f]The change of proton density (%)
[g]The change of electron temperature (%)
[h]The change of proton temperature (%)

angle θ between the axis of the MC, adopted by fitting the constant α force-free model to the magnetic fields, and its leading shock normal is in the range from 65 to 115 degree; and (2) the interval t between the shock and the beginning of the MC is less than 14 h. The final 23 events are listed in Table 5.2.

5.3 Statistical Results

It can be seen from Tables 5.1 and 5.2 that the magnetic field decreases (ΔBt $\sim$ −20.1 %) in most of the RE events and plasma is usually compressed (ΔNp $\sim$ 35.6 %) and heated (ΔTe $\sim$ 10.6 %, ΔTp $\sim$ 27.1 %). These phenomena resemble those of the BL results as previously discussed in Chap. 4. In addition, the absolute difference of proton velocity in the RE (ΔVp $\sim$ 21.7 km/s) is larger than that in the BL (ΔVp $\sim$ 12.1 km/s). The MC-driven shocks are usually fast forward shocks across which the magnetic field, proton and electron temperature, and plasma speed always increase apparently (the average changes of ΔBt, ΔNp, ΔTe, ΔTp, ΔVp are $\sim$140.7, 122.2, 82.9, 161.3 %, and 81.5 km/s, respectively). It is also noted that there are few strong MC-driven shocks. The obtained density compression ratio of the shock is in the range of 1.3–4.6 with a mean value of only 2.2.

Figure 5.1 displays the electron flux variation ΔF averaged over all events in the parallel, antiparallel, and perpendicular directions as well as the omni proton flux variation also averaged over all events. The flux variations (flux decrease or increase) depend both on the direction and the energy. Inside the RE, the core electron flux in the parallel and antiparallel direction increases consistently and the increment amplitude decreases with energy monotonously from $\sim$30 % (at 18 eV)

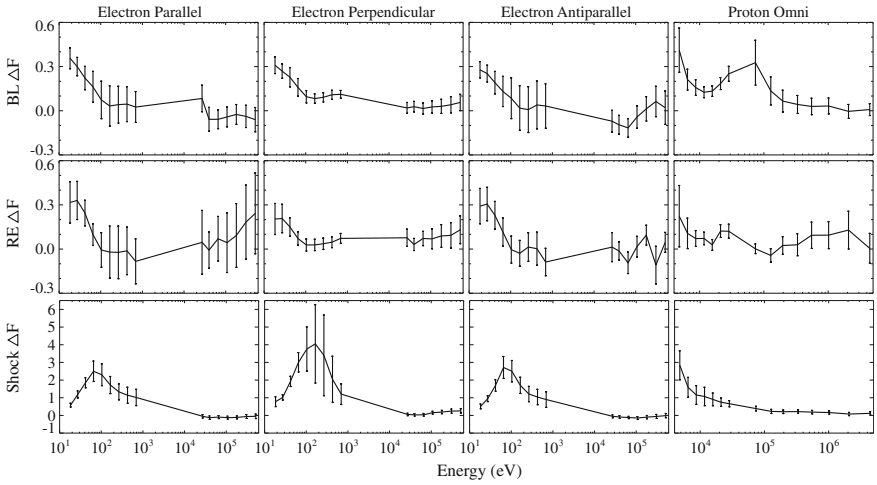

Fig. 5.1 Normalized mean flux variations with error bars at each energy band. *First row* BL; *second row* RE; *third row* MC-driven shock; *first column* electron flux in the parallel direction; *second column* electron flux in the perpendicular direction; *third column* electron flux in the antiparallel direction; *fourth column* proton flux in the omnidirection

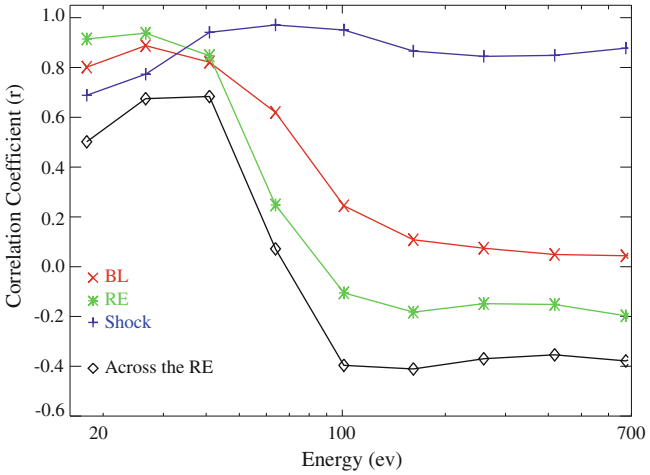

Fig. 5.2 Correlation coefficients of electron increments in the parallel and antiparallel directions. In the BL: *red*, in the RE: *green*, across the MC-driven shock: *blue*, across the RE: *black*

to $\sim$10 % (at 70 eV); the increments of suprathermal electron (100–700 eV) in the parallel and antiparallel directions are very small (<4 %), but it is noted that their standard errors are obviously large. Although the energetic electron in the parallel direction has higher increment with larger standard error, the flux variations in the RE have similar behaviors compared with the BL as a whole. By contrast, across the shock, flux behaviors are quite different. The electron flux variations have peak increments (>200 %) around $\sim$100 eV and decline on both sides; we also note that they have higher increments in the perpendicular direction and the corresponding energy of the peak increment is also higher in the perpendicular direction ($\sim$165 eV) than in the field-aligned direction ($\sim$65 eV); the omni proton flux increments decrease monotonously from $\sim$280 % (at 4 keV) to $\sim$10 % (at 4 MeV).

Similar to the results discussed in Chap. 4, it is also found that the correlations of the electron flux variations in parallel and antiparallel directions have a sharp change around 70 eV in the RE. Figure 5.2 shows the correlation coefficients of electron flux variations in the parallel and antiparallel directions. In all events, the core electron has (strong) positive correlations (BL and RE: $r > 0.8$; shock: $r > 0.6$); while the suprathermal electron in the BL and RE has low or negative correlations (BL: $r \sim 0$; RE: $r \sim -0.2$). In addition, the correlations are even lower across (downstream to upstream) the RE ($r \sim -0.4$), however, no obvious changes are found across the shock which always has high correlation around 0.8.

5.4 Explanations for the Flux Variations in Different Events

5.4.1 *The Magnetic Cloud Boundary Layer and Reconnection Exhaust*

The statistical results show that plasma in the BL and RE are both compressed and heated, and they have similar macroscopical variations in plasma density, temperature, and velocity. Whereas in microcosmical view, the flux enhancements of the core electrons and suprathermal electrons in RE are also similar to those in the BL. Such similarities tend to reveal that the BL and RE are dominated by the same physical processes, and magnetic reconnection is the candidate one.

Here we would like to explain why these features are related to the solar wind reconnection in detail. As sketched in Fig. 5.3, taking the Strahl electron in ideal case for instance, the intensity of flux is simply normalized by only two arbitrary quantities: 100 (obvious Strahl electron) and 10 (no obvious Strahl electron). The flux status is described by [F0, F180], where F0 and F180 stand for the flux of Strahl electron in the parallel and antiparallel directions, respectively. Accordingly, the status of bidirectional Strahl electron, unidirectional Strahl electron in the parallel and antiparallel directions and no obvious Strahl electron could be described by [100, 100], [100, 10], [10, 100] and [10, 10], respectively. In case I,

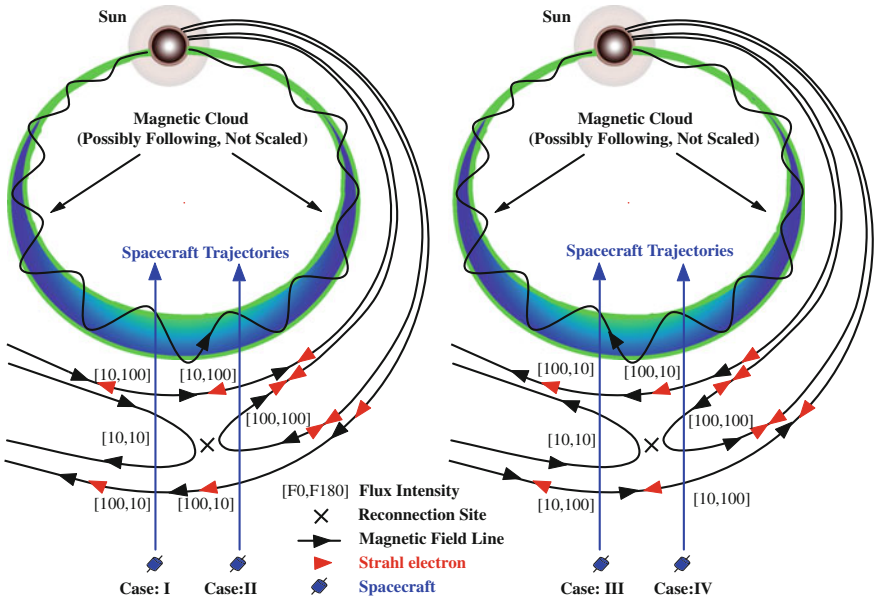

Fig. 5.3 Schematic plot of magnetic field disconnection (possible reconnection) of four cases and the possibly following MC

the spacecraft would detect decreased and unchanged Strahl electron in the parallel and antiparallel directions, respectively, inside the RE, and the increments are [−90, 0] ([10, 10]–[100, 10]). Similarly, the increments in cases II, III, and IV are [0, 90], [0, −90], and [90, 0], respectively. Therefore, in statistical analyses, the correlations of the Strahl electron flux variations in parallel and antiparallel directions should be low if the spacecraft encounter the above four cases randomly. Mathematically speaking, both the correlation coefficient and the averaged increments should approach 0. Moreover, across the RE, the increments become [−90, 90] in cases I, II and [90, −90] in cases III, IV. We could see that they always reveal anticorrelated relations in the parallel and antiparallel directions. Accordingly, the theoretically computed correlation coefficient is even lower (should be −1) in the statistical work.

Certainly, our assumptions are relatively simple. For example, the real flux intensity could not be only two quantities (100 and 10), and thus the finally obtained correlation coefficients and mean flux increments might not be as ideal as those in the analyses. However, the flux variations of suprathermal electron still reveal the properties that the mean increments approach 0with large standard errors and the correlation coefficients are low (~ -0.2) and lower (~ -0.4) in and across the RE. Other effects, such as particle scattering, could also modify the flux of electron. If so, it should be explained as to why the correlation of core electron is always higher than the suprathermal electron and why the correlation coefficients change sharply around $\sim$70 eV. Perhaps the correlation coefficients should change more smoothly if the scattering process plays a dominant role. In addition, since these RE events are not magnetically connected to Earth's bow shock (Huttunen et al. 2007), the obtained results would not be greatly affected by particle reflection either. Moreover, the correlation coefficients across the MC-driven shock, in which there is no obvious break or reverse of magnetic field line, are always high ($\sim$0.7–0.9). For these reasons, we tend to regard that the solar wind magnetic reconnection is the best candidate process that could account for the statistically obtained low or negative correlations of suprathermal electron increments in the parallel and antiparallel directions.

5.4.2 *The MC-Driven Shock*

Particle flux variations are totally different across the MC-driven shocks compared with those in the BL and RE. The electron flux increments ascend first and then descend with peak value near $\sim$65 and $\sim$165 eV in the field-aligned and perpendicular directions, respectively. Such flux behaviors could not be merely caused by the density increase and increments are also inconsistent with the average density increments. We noted that the increase of electron temperature across the shock is quite higher than that in the BL and RE. Since the "moment temperature" is calculated from the second-order moment of the VDF, we speculate that the increments of electron flux with hill-like shape are mainly dominated by the heating effect of the shock. As seen in Fig. 5.4, higher temperature will broaden the particle

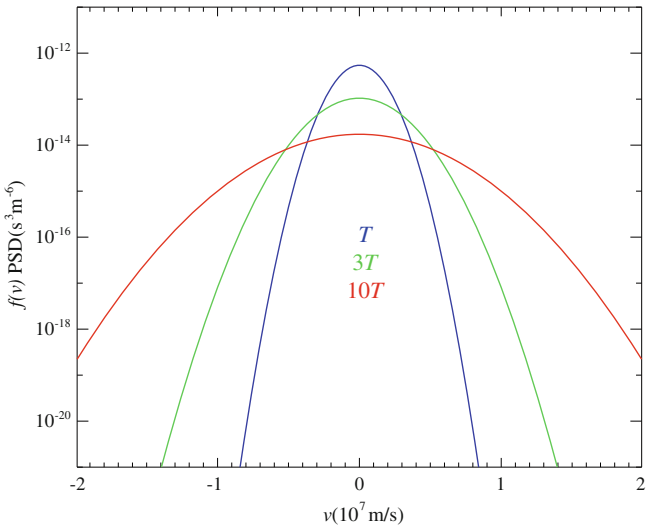

Fig. 5.4 VDF with temperature (T, 3T, 10T) under the same density condition

VDF even if they have the same density. This result is consistent with previous observations which show that the inflated electron VDF caused by heating in both the parallel and perpendicular directions is always found downstream of the shock (Fitzenreiter et al. 2003). In addition, according to early researches, for weaker shocks, the electron heating was primarily perpendicular to the magnetic field due to the conservation of magnetic moment (Feldman et al. 1983). The present statistical results with higher flux increments in the perpendicular directions could also be supported by such explanations, since many of our selected MC-driven shocks have relatively small density compression ratio. Since the proton flux increment ($\sim$280 %) across the MC-driven shock at 4 keV is higher than both the density and temperature increments ($\sim$122 and 161 %, respectively), it is speculated that the proton VDF around 4 keV might also be inflated as that of the electron near $\sim$70 eV across the shock.

5.5 Discussion and Summary

Magnetic field decrease, and density and temperature increase are similar in the RE and BL, and similar flux variation behaviors are found between these two structures. Hence, we suggest that the flux variations in the BL are mainly related to the magnetic reconnection process. However, as preliminarily discussed in the introduction section, some researchers pointed out that the roughly Alfvénic accelerated plasma flows: the "direct evidence" (Gosling 2011; Gosling et al. 2005a), are rarely identified inside the front BL (except two events: 20001003 and 20040724).

At first, it should be recognized that when there is no roughly Alfvénic accelerated plasma flows it does not mean that there is no magnetic reconnection, since the reconnection jets might not be measured or the generated jets do not meet the referred criteria. Previous simulations (Wang et al. 2010, 2003a, b) imply that the BL has strong turbulent property under high magnetic Reynolds number condition ($\mathrm{Rm} \sim 10^4$). While, as also suggested by Matthaeus et al. (2003), turbulence should commonly drive reconnection in the solar wind. Inside the BL, the compression of the MC behaves as driving flows that would reduce the characteristic thickness of the local current sheet from $\sim 10^8$ km (in the corona) to $\sim 10^3$ km (in the solar wind). Accordingly, the magnetic Reynolds number could decrease from $\sim 10^{10}$ to $\sim 10^4$. Besides, the magnetic field inside the BL always shows abrupt deflections in the field direction. If the frozen field theorem is locally broken, these conditions are all favored by the potential magnetic reconnection (Wei et al. 2006).

Actually, in many cases, the BL is a complex layer with turbulent and irregular structures. Besides, the trajectory of the spacecraft relative to the orientation of RE is not always suitable for the observation. So, the roughly Alfvénic accelerated plasma flows that completely meet the reconnection criteria as those reported events might be hard to identify. In addition, the referred criteria, especially the jets (Gosling 2011; Gosling et al. 2005a; Paschmann et al. 1986; Sonnerup and Cahill 1967; Sonnerup et al. 1981), are described as "a useful guide" (Sonnerup et al. 1981) for the identification of reconnection and have made wonderful achievements in the realm of magnetic reconnection. Yet it should still be cautious to use such criteria because they are obtained under the MHD descriptions with the assumption of ideal reconnection model. Remarkably, it is pointed out that such criteria have never been demonstrated to be "incontrovertible" (Sonnerup et al. 1981). Recent simulations also show that the outflowing reconnection jets could even turn back and link with the inflows to form closed-circulation patterns in turbulent reconnection (Lapenta 2008). Accordingly, reconnection generated plasma flows might not meet the referred criteria strictly in the real three-dimensional space. Therefore, it is quite possible that many reconnections inside the BL do occur and the reconnection jets are indeed measured. However, they are excluded by the criteria so that many researchers tend to think that there is no reconnection.

Other factors should also be taken into consideration carefully, such as the lifespan and the evolution of the reconnection itself. As studied previously (Wei et al. 2003a, b), the magnetic reconnection might not be an ongoing process all the time. After the reconnection occurs, the reconnection conditions would be weakened and the frozen-in condition would be gradually recovered until the local condition is ready for the next potential magnetic reconnection. Since this process might continue to repeat itself, a single spacecraft across the BL might observe the "'remains" or the "preorder" of magnetic reconnection. For these reasons, the signatures of reconnection, such as the Alfvénic accelerated flows, might not be prominent to be identified sometimes. However, we have reasons to believe that the electron flux variations would not be affected and could reflect the field topological structure of the magnetic reconnection event to a certain extent.

In summary, we carry out a statistical study to analyze the proton and electron flux variations inside BL events on reliable energy bands and compare them with those in the RE and across the MC-driven shocks. The results show that the BL is a unique complicated transition layer that displays some reconnection characteristics. The core electron flux behaviors inside the BL and RE are related to the density increase. The hill-like electron flux increments across the shock are mainly dominated by the temperature increase. It is also found that the correlations of the electron flux variations in parallel and antiparallel directions have a sharp change around $\sim$70 eV where solar wind magnetic reconnection occurs. The correlation coefficients of the suprathermal electron in the parallel and antiparallel directions are found to be low. Further analyses imply that strong energy dependence and direction selectivity of flux variations could be regarded as an important signature of solar wind reconnection in the statistical point of view.

References

Birn, J., Priest, E.R.: Reconnection of Magnetic Fields: Magnetohydrodynamics and Collisionless Theory and Observations. Cambridge University Press, (2007)

Dasso, S., Mandrini, C.H., Démoulin, P., Luoni, M.L.: A new model-independent method to compute magnetic helicity in magnetic clouds. A&A **455**(1), 349–359 (2006). doi:10.1051/0004-6361:20064806

Davis, M.S., Phan, T.D., Gosling, J.T., Skoug, R.M.: Detection of oppositely directed reconnection jets in a solar wind current sheet. Geophys. Res. Lett. **33**(19), L19102 (2006). doi:10.1029/2006gl026735

Feldman, W.C., Anderson, R.C., Bame, S.J., Gosling, J.T., Zwickl, R.D., Smith, E.J.: Electron velocity distributions near interplantary shocks. J. Geophys. Res. **88**(A12), 9949–9958 (1983). doi:10.1029/JA088iA12p09949

Feng, H.Q., Wu, D.J., Chao, J.K., Lee, L.C., Lyu, L.H.: Are all leading shocks driven by magnetic clouds? J. Geophys. Res. **115**(A4), A04107 (2010). doi:10.1029/2009ja014875

Fitzenreiter, R.J., Ogilvie, K.W., Bale, S.D., Viñas, A.F.: Modification of the solar wind electron velocity distribution at interplanetary shocks. J. Geophys. Res. **108**(A12), 1415 (2003). doi:10.1029/2003ja009865

Gosling, J.T.: Magnetic reconnection in the solar wind. Space Sci. Rev. 1–14 (2011). doi:10.1007/s11214-011-9747-2

Gosling, J.T., Eriksson, S., Blush, L.M., Phan, T.D., Luhmann, J.G., McComas, D.J., Skoug, R. M., Acuna, M.H., Russell, C.T., Simunac, K.D.: Five spacecraft observations of oppositely directed exhaust jets from a magnetic reconnection X-line extending > 4.26×10^6 km in the solar wind at 1 AU. Geophys. Res. Lett. **34**(20), L20108 (2007a). doi:10.1029/2007gl031492

Gosling, J.T., Phan, T.D., Lin, R.P., Szabo, A.: Prevalence of magnetic reconnection at small field shear angles in the solar wind. Geophys. Res. Lett. **34**(15), L15110 (2007b). doi:10.1029/2007gl030706

Gosling, J.T., Skoug, R.M., McComas, D.J., Smith, C.W.: Direct evidence for magnetic reconnection in the solar wind near 1 AU. J. Geophys. Res. **110**(A1), A01107 (2005a). doi:10.1029/2004ja010809

Gosling, J.T., Skoug, R.M., McComas, D.J., Smith, C.W.: Magnetic disconnection from the Sun: observations of a reconnection exhaust in the solar wind at the heliospheric current sheet. Geophys. Res. Lett. **32**(5), L05105 (2005b). doi:10.1029/2005gl022406

Huttunen, K.E.J., Bale, S.D., Phan, T.D., Davis, M., Gosling, J.T.: Wind/WAVES observations of high-frequency plasma waves in solar wind reconnection exhausts. J. Geophys. Res. **112**(A1), A01102 (2007). doi:10.1029/2006ja011836

Lapenta, G.: Self-feeding turbulent magnetic reconnection on macroscopic scales. Phys. Rev. Lett. **100**(23), 235001 (2008). doi:10.1103/PhysRevLett.100.235001

Lavraud, B., Gosling, J., Rouillard, A., Fedorov, A., Opitz, A., Sauvaud, J.A., Foullon, C., Dandouras, I., Génot, V., Jacquey, C., Louarn, P., Mazelle, C., Penou, E., Phan, T., Larson, D., Luhmann, J., Schroeder, P., Skoug, R., Steinberg, J., Russell, C.: Observation of a complex solar wind reconnection exhaust from spacecraft separated by over 1800 RE. Sol. Phys. **256**(1), 379–392 (2009). doi:10.1007/s11207-009-9341-x

Matthaeus, W.H., Dmitruk, P., Oughton, S., Mullan, D.: Turbulent dissipation in the solar wind and corona. In: AIP Conference Proceedings **679**(1), 427–432 (2003). doi:10.1063/1.1618627

McComas, D.J., Gosling, J.T., Hammond, C.M., Moldwin, M.B., Phillips, J.L., Forsyth, R.J.: Magnetic reconnection ahead of a coronal mass ejection. Geophys. Res. Lett. **21**(17), 1751–1754 (1994). doi:10.1029/94gl01077

Paschmann, G., Papamastorakis, I., Baumjohann, W., Sckopke, N., Carlson, C.W., Sonnerup, B.U. Ö., Lühr, H.: The magnetopause for large magnetic shear: AMPTE/IRM observations. J. Geophys. Res. **91**(A10), 11099–11115 (1986). doi:10.1029/JA091iA10p11099

Phan, T.D., Gosling, J.T., Davis, M.S., Skoug, R.M., Oieroset, M., Lin, R.P., Lepping, R.P., McComas, D.J., Smith, C.W., Reme, H., Balogh, A.: A magnetic reconnection X-line extending more than 390 Earth radii in the solar wind. Nature **439**(7073), 175–178 (2006). doi:10.1038/nature04393

Sonnerup, B.U.Ö., Cahill Jr, L.J.: Magnetopause structure and attitude from explorer 12 observations. J. Geophys. Res. **72**(1), 171–183 (1967). doi:10.1029/JZ072i001p00171

Sonnerup, B.U.Ö., Paschmann, G., Papamastorakis, I., Sckopke, N., Haerendel, G., Bame, S.J., Asbridge, J.R., Gosling, J.T., Russell, C.T.: Evidence for magnetic field reconnection at the Earth's magnetopause. J. Geophys. Res. **86**(A12), 10049–10067 (1981). doi:10.1029/JA086iA12p10049

Tian, H., Yao, S., Zong, Q., He, J., Qi, Y.: Signatures of magnetic reconnection at boundaries of interplanetary small-scale magnetic flux ropes. Astrophys. J. **720**(1), 454 (2010). doi:10.1088/0004-637X/720/1/454

Wang, Y., Wei, F.S., Feng, X.S., Zhang, S.H., Zuo, P.B., Sun, T.R.: Energetic electrons associated with magnetic reconnection in the magnetic cloud boundary layer. Phys. Rev. Lett. **105**(19), 195007 (2010). doi:10.1103/PhysRevLett.105.195007

Wei, F.S., Feng, X., Yang, F., Zhong, D.: A new non-pressure-balanced structure in interplanetary space: boundary layers of magnetic clouds. J. Geophys. Res. **111**(A3), A03102 (2006). doi:10.1029/2005ja011272

Wei, F.S., Hu, Q., Feng, X., Fan, Q.: Magnetic reconnection phenomena in interplanetary space. Space Sci. Rev. **107**(1), 107–110 (2003a). doi:10.1023/a:1025563420343

Wei, F.S., Liu, R., Fan, Q., Feng, X.: Identification of the magnetic cloud boundary layers. J. Geophys. Res. **108**(A6), 1263 (2003b). doi:10.1029/2002ja009511

Xu, X., Wei, F., Feng, X.: Observations of reconnection exhausts associated with large-scale current sheets within a complex ICME at 1 AU. J. Geophys. Res. **116**(A5), A05105 (2011). doi:10.1029/2010ja016159

Chapter 6
Summary and Outlook

In this thesis, we carry out some researches related to magnetic reconnection and particle acceleration in the BL. The main conclusions are (1) we observe the energetic electrons associated with magnetic reconnection in the solar wind for the first time; (2) we propose a combined acceleration model to explain how the energetic electrons are accelerated in magnetic reconnection processes; (3) we reveal the energy dependency and direction selectivity of particle flux variations in the BL; (4) we indicate that particle flux variations could be considered as an important signature of solar wind reconnection in the statistical point of view.

As discussed in the previous chapters, detailed observation of reconnection diffusion region is the crucial point through which we can have better understandings of the physical processes related to magnetic reconnection (Birn and Priest 2007). Hence, the following aspects should be noted: (1) seeking the reconnection diffusion region in the solar wind; (2) using more self-consistent PIC simulations to discuss the particle accelerations in magnetic reconnection; (3) investigating the rear BL of the MC to have more comprehensive understandings of the BL dynamics; (4) trying to find a more convenient and efficient method to identify the reconnection event in the solar wind.

Actually, turbulence and waves are commonly observed in magnetic reconnection processes (Birn and Priest 2007; Biskamp 2003; Deng and Matsumoto 2001; Eastwood et al. 2009; Farrell et al. 2002; Matthaeus and Velli 2011; Matthaeus et al. 2003). The relation between magnetic reconnection and turbulence is an important and frontier topic in space physics. It should also be noted that the reconnection current sheets can be produced by turbulence, and conversely, turbulence can also be generated by magnetic reconnection (Karimabadi et al. 2013; Liu et al. 2013; Eastwood et al. 2009; Servidio et al. 2009, 2010; Retino et al. 2007). In addition, waves associated with reconnection may play an important role in the initiation and evolution of magnetic reconnection. Wave−particle interactions are also important in the dissipation of turbulence (Bale et al. 2005; Howes et al. 2011; TenBarge et al. 2013; Tu and Marsch 1995). Therefore, the future work will be investigations on the relations among magnetic reconnection, turbulence, and waves together with their interactions.

© Springer-Verlag Berlin Heidelberg 2016

Y. Wang, *Magnetic Cloud Boundary Layers and Magnetic Reconnection*,
Springer Theses, DOI 10.1007/978-3-662-48310-7_6

References

Bale, S.D., Kellogg, P.J., Mozer, F.S., Horbury, T.S., Reme, H.: Measurement of the electric fluctuation spectrum of magnetohydrodynamic turbulence. Phys. Rev. Lett. **94**(21), 215002 (2005). doi:10.1103/PhysRevLett.94.215002

Birn, J., Priest, E.R.: Reconnection Of Magnetic Fields: Magnetohydrodynamics and Collisionless Theory and Observations. Cambridge University Press, (2007)

Biskamp, D.: Magnetohydrodynamic Turbulence. Cambridge University Press, Cambridge (2003)

Deng, X.H., Matsumoto, H.: Rapid magnetic reconnection in the Earth's magnetosphere mediated by whistler waves. Nature **410**(6828), 557–560 (2001). doi:10.1038/35069018

Eastwood, J.P., Phan, T.D., Bale, S.D., Tjulin, A.: Observations of turbulence generated by magnetic reconnection. Phys. Rev. Lett. **102**(3), 035001 (2009). doi:10.1103/PhysRevLett.102.035001

Farrell, W.M., Desch, M.D., Kaiser, M.L., Goetz, K.: The dominance of electron plasma waves near a reconnection X-line region. Geophys. Res. Lett. **29**(19), 1902 (2002). doi:10.1029/2002gl014662

Howes, G.G., TenBarge, J.M., Dorland, W., Quataert, E., Schekochihin, A.A., Numata, R., Tatsuno, T.: Gyrokinetic Simulations of Solar Wind Turbulence from Ion to Electron Scales. Phys. Rev. Lett. **107**(3), 035004 (2011)

Karimabadi, H., Roytershteyn, V., Daughton, W., Liu, Y.-H.: Recent evolution in the theory of magnetic reconnection and its connection with turbulence. Space Science Reviews, 1–17 (2013). doi:10.1007/s11214-013-0021-7

Liu, Y.-H., Daughton, W., Karimabadi, H., Li, H., Roytershteyn, V.: Bifurcated structure of the electron diffusion region in three-dimensional magnetic reconnection. Phys. Rev. Lett. **110**(26), 265004 (2013)

Matthaeus, W., Velli, M.: Who needs turbulence? Space Sci. Rev. **160**(1), 145–168 (2011). doi:10.1007/s11214-011-9793-9

Matthaeus, W.H., Dmitruk, P., Oughton, S., Mullan, D.: Turbulent dissipation in the solar wind and corona. AIP Conf. Proc. **679**(1), 427–432 (2003). doi:10.1063/1.1618627

Retino, A., Sundkvist, D., Vaivads, A., Mozer, F., Andre, M., Owen, C.J.: In situ evidence of magnetic reconnection in turbulent plasma. Nat. Phys. **3**(4), 236–238 (2007)

Servidio, S., Matthaeus, W.H., Shay, M.A., Cassak, P.A., Dmitruk, P.: Magnetic reconnection in two-dimensional magnetohydrodynamic turbulence. Phys. Rev. Lett. **102**(11), 115003 (2009)

Servidio, S., Shay, M.A., Matthaeus, W.H., Dmitruk, P., Cassak, P.A., Wan, M.: Properties of magnetic reconnection in MHD turbulence. AIP Conf. Proc. **1216**(1), 198–201 (2010)

TenBarge, J.M., Howes, G.G., Dorland, W.: Collisionless damping at electron scales in solar wind turbulence. Astrophys J **774**(2), 139 (2013)

Tu, C.Y., Marsch, E.: MHD structures, waves and turbulence in the solar wind: observations and theories. Space Sci. Rev. **73**(1), 1–210 (1995). doi:10.1007/bf00748891